Developing gold- and silver-catalyzed dehydrogenative cross-coupling toward donor-acceptor polymer synthesis

Lauren Kang

A dissertation

submitted in partial fulfillment of the

requirements for the degree of

Doctor of Philosophy

University of Washington

2018

Reading Committee:

Christine K. Luscombe, Chair

Gojko Lalic

Alshakim Nelson

Program Authorized to Offer Degree:

Chemistry

University of Washington

Abstract

Developing gold- and silver-catalyzed dehydrogenative cross-coupling toward donor-acceptor polymer synthesis

Lauren June Kang

Chair of the Supervisory Committee:
Professor Christine K. Luscombe
Materials Science & Engineering

π-Conjugated polymers are materials of interest for use in organic electronics. Within these polymers, donor-acceptor polymers are favorable for solar cell applications due to improved charge mobility, better absorption in the low energy region of the solar spectrum, and tunable band gaps. One of the barriers to commercializing these donor-acceptor materials is that their synthetic pathways are complex because of the alternating repeat units in the polymer. To address this, the applications of cross dehydrogenative coupling (also called oxidative CH/CH cross-coupling) toward the synthesis of donor-acceptor polymers was explored. In this work, the roles of specific reagents in a one-pot gold- and silver-catalyzed cross dehydrogenative coupling and the factors that contribute to selectivity for cross-coupling rather than homo-coupling are elucidated. Based on our results, we conclude that the difference in rate of C-H activation by gold and silver dominate the percentage of alternating repeat units in the final polymer, which may be exploited to control the ratio of electron-rich to electron-poor monomers.

TABLE OF CONTENTS

List of Figures iv

List of Tables vi

Chapter 1. Introduction of Donor-Acceptor Polymers 1

1.1 Introduction 1

1.2 Examples of d-a polymers for OPV 2

1.2.1 Thieno[3,4-b]thiophene based polymers 2

1.2.2 Diketopyrrolopyrrole based polymers 4

1.2.3 Benzothiadiazole and difluorobenzothiadiazole based polymers 5

1.3 Cost analysis of OPV materials 7

1.4 Conclusion 8

Chapter 2. Recent Developments in C–H Activation for Materials Science in the Center for Selective C–H Activation 9

2.1 Introduction 9

2.2 Direct Arylation of Electron-Poor π-Conjugated Small Molecules 10

2.3 Earth-Abundant Metal-Initiated Iodination 17

2.4 Toward Living Polymerizations to Synthesize Semiconducting Polymers Using Poly(3-hexylthiophene) as the Model Polymer 20

2.5 Conclusions and Outlook 25

Chapter 3. Exploration and development of gold- and silver-catalyzed dehydrogenative cross-coupling toward donor-acceptor polymer synthesis 26

3.1 Introduction 26
3.2 Results and Discussion 28
3.2.1 Preliminary small molecule screening 28
3.2.2 Electronic effect on polymerization 32
3.2.3 Cross-coupling mechanism studies 33
3.2.4 Deuterium Studies 35
3.2.5 Kinetic effects on polymerization 38
3.3 Conclusions 39
3.4 Experimental 40
3.4.1 General procedures and materials 40
3.4.2 Cross-coupling studies 40
3.4.3 Deuterium studies 41
3.4.4 Dehydrogenative Cross-coupling Polymerization 41
3.4.5 Slow Thiophene Addition Dehydrogenative Cross-coupling Polymerization 42
3.5 Future Work 42
3.5.1 Explore one-pot polymerization kinetic controls 42
3.5.2 Target specific sequences of monomer incorporation 43
3.5.3 Combine findings for 95% alternation D-A polymer 43
Bibliography 44
Appendix A 50
Chapter 4. Supplementary Information for Chapter 3 50
4.1 General procedures 50

4.2 Calculation of Deuterium Integration % 51
4.3 Reaction Progress Kinetics Analysis (RPKA) – Same Excess[117] 51
4.4 Spectral Data 53
4.4.1 MALDI data 53
4.4.2 ^{1}H NMR 55
4.5 Calculating % alt and M_n using ^{1}H NMR 57
Appendix B 58
Chapter 5. Poly(3-hexylthiophene) end-functionalization via quenching resulting in heteroatom-bond formation. 58
5.1 Abstract 58
5.2 Introduction 58
5.3 Results and Discussion 64
5.4 Conclusion 66
PROFESSIONAL EXPERIENCE 67
LEADERSHIP & CIVIC ACTIVITIES 68
COMMUNICATION 69

LIST OF FIGURES

Figure 1.1. Structures of thieno[3,4-b]thiophene based polymers. 3

Figure 1.2. Structures of diketopyrrolopyrrole based polymers..... 5

Figure 1.3. Structures of benzothiadiazole based polymers. 7

Figure 2.1. Strong electron acceptors for C–H activation with selected aryl halide substrates. 15

Figure 2.2. π-Conjugated materials synthesized by C–H activated direct arylation similar to that reported in Figure 2.1. 17

Figure 2.3. Potassium *tert*-butoxide initiated C–H iodination of electron-deficient heteroaromatic compounds. 18

Figure 2.4. Materials constructed using C–H iodination methodology for application in organic photovoltaics. 20

Figure 2.5. Proposed dual-metal catalyzed poly(3-hexylthiophene) (P3HT) synthesis. 23

Figure 2.6. Polymerization of aurylated thiophene species. 23

Figure 2.7. One-pot dual-catalytic silver and palladium polymerization..... 24

Figure 3.1. Synthetic pathways for donor-acceptor polymers. 27

Figure 3.2. Proposed mechanism for Au(I) and Au(III) catalyzed CDC. **A** represents the electron-poor (acceptor) monomer and **D** represents the electron-rich (donor) monomer. 28

Figure 3.3. Scheme of small molecule dehydrogenative cross-coupling reaction. 29

Figure 3.4. Polymerization reaction scheme with 1,2,4,5-tetrafluorobenzene (polymerization 1) and with 2,2',3,3',5,5',6,6'-octafluorobiphenyl (polymerization 2) as the electron-poor monomer. All polymerizations were run on a 1 mmol scale with 1:1 comonomer ratios. 31

Figure 3.5. Example ^{1}H NMR showing region used for % alt calculation. The ^{1}H NMR corresponds to Polymer 2 in $CDCl_3$ at 192 h timepoint..... 32

Figure 3.6. Scheme of deuterium study of pentafluorobenzene. 36

Figure 3.7. Scheme of deuterium study of 2-methylthiophene. 37

Figure 3.8. Simplified proposed mechanism of gold- and silver-catalyzed dehydrogenative cross-coupling. 38
Figure 4.1. Example 2H NMR of deuterated product. 51
Figure 4.2. Reaction scheme for reaction progress kinetics analysis. 52
Figure 4.3. [A] vs. Reaction time plots overlay. 53
Figure 4.4. Polymer 1 53
Figure 4.5. Polymer 2 54
Figure 4.6. Example NMR spectrum of Polymer 1 55
Figure 4.7. Region of NMR spectrum used to calculate % alt and M_n. 56
Figure 5.1. Kumada Catalyst-Transfer Polycondesation Mechanism. 60
Figure 5.2. General schemes of three methods of end-functionalizing P3HT: initiators, quenchers, and post-polymerization. 62
Figure 5.3. Mono and bis-thiol end-functionalization of P3HT. 65
Figure 5.4. Combination of initiator and quencher to yield discrete functionalities on either end of P3HT 66

LIST OF TABLES

Table 3.1. Optimization of small molecule cross-coupling reaction..... 30
Table 3.2. Results of polymerization reaction comparing 1,2,4,5-tetrafluorobenzene to 2,2',3,3',5,5',6,6'-octafluorobiphenyl as the electron-poor monomer. 33
Table 3.3. Control experiments for dehydrogenative cross-coupling reaction. 34
Table 3.4. Deuterium study results of pentafluorobenzene..... 36
Table 3.5. Deuterium study results of 2-methylthiophene. 37
Table **3.6**. Slow addition of thiophene studies. 39
Table 4.1. Notable M/Z values observed from MALDI of Polymer 1..... 53
Table 4.2. Notable M/Z values observed from MALDI of Polymer 2..... 54

ACKNOWLEDGEMENTS

I would like to acknowledge the support from the Luscombe research group. I have become a better scientist through the help of my PI, past post-docs, and my fellow graduate students. I would especially like to thank my PI, Prof. Christine Luscombe, for her support and guidance. I also want to thank Dr. Sabin-Lucian Suraru, who helped in my early graduate years. I want to thank Dr. Jason Lee for helping throughout my time at UW and for always being a guiding light in my scientific pursuits.

Both the Clean Energy Institute and the Center for Selective C-H Functionalization have played crucial roles in making my graduate school experience a well-rounded one.

I would like to thank my family and friends for their support. I would not have been able to even dream of coming to graduate school without the undying support and love that I have received from my parents. My sisters and brother-in-law have also sent endless amounts of encouragement and for that I am grateful.

Last, but not least, I want to thank Rob for being a great partner throughout the whole length of my graduate school career.

DEDICATION

I dedicate this dissertation to my parents.

Chapter 1. INTRODUCTION OF DONOR-ACCEPTOR POLYMERS

1.1 INTRODUCTION

In the organic electronics field, a class of materials of growing interest is donor-acceptor polymers, which consist of at least two alternating moieties: one that is electron-rich and one that is electron-poor. They are especially of interest as p-type materials for solar cell applications. The alternation of electron-rich and electron-poor moieties, as compared to more classic p-type materials such as poly-(3-hexylthiophene), results in improved charge transport, tunable band gaps, and improved absorption in lower energy levels.

The two main mechanisms that are responsible for the lower bandgap (E_g) of D–A polymers are the delocalization of electrons along the polymer backbone and hybridization of molecular orbitals. First, the D–A structure aids the delocalization of electrons along the conjugated backbone, which helps to stabilize the quinoid structure over the backbone, leading to a smaller energy gap.[1] Second, hybridization of frontier molecular orbitals can further reduce the energy gap. According to the rules of perturbation theory, the HOMO of the donor segment will interact with the HOMO of the acceptor segment to yield two new HOMOs for the D−A polymer. Similarly, the LUMO of the donor will interact with that of the acceptor to produce two new LUMOs of the D−A polymer.[2] Once the electrons are redistributed, a new set of HOMO and LUMO levels of the bonded compound is produced, which results in a smaller bandgap. This concept also explains the fact that for the D–A polymer, the resulting HOMO level is largely affected by the donor, and the LUMO is largely affected by the acceptor.[3] Recent studies suggest that these two mechanisms are closely related and could be mutually beneficial.[4]

Synthesizing D–A polymers traditionally starts by forming a C–C bond between two functionalized moieties. Transition metal-catalyzed cross-coupling reactions, such as Sonogashira, Heck, Suzuki–Miyaura or Stille reactions, or direct arylation couplings, are used to form such bonds.[3,5,6] The first design consideration for a D–A OPV polymer is the bandgap, which depends largely on the strength of the electron-pushing and pulling abilities of the donor and acceptor. The HOMO and LUMO energy levels of a polymer are of crucial importance because they are directly linked to the open-circuit voltage (V_{oc}) and the charge-separation efficiency of the organic photovoltaic (OPV). When designing a p-type photovoltaic polymer, it is best to downshift the HOMO level while keeping the LUMO level above that of the n-type material.[7] Good solubility in common organic solvents is also needed for solution processing, which can be affected by factors such as molecular weight, side-chains, rigidity of the polymer backbone and the strength of the polymers' intermolecular interaction.[8] Here in we will discuss a few examples of donor-acceptor polymers that have pushed the OPV field forward.

1.2 Examples of D-A polymers for OPV

1.2.1 *Thieno[3,4-b]thiophene based polymers*

Thieno[3,4-*b*]thiophene (TT) units were introduced in 2009 as a strong acceptor unit in OPV.[9,10] TT units were copolymerized with the benzo[1,2-*b*:4,5-*b'*]dithiophene (BDT) unit, giving a series of polymers with bandgaps of ~1.6 eV.[11] A milestone in OPV technology was achieved with a solar cell based on the copolymer PTB7 (Figure 1.1, Polymer 1), containing BDT and TT units, with diiodooctane as an additive for morphology tuning, which exhibited a power conversion efficiency (PCE) of 7.4% without device architecture optimization.[10] This high PCE is believed to be related to the high planarity of the BDT unit, the low-lying HOMO

caused by fluorine, and an appropriate side-chain length which effects the polymer molecular mass and solubility.[12–14] This family of polymers has pushed the field forward through different chemical modifications, such as adding in aromatic spacers.[15,16] Substantial improvements in the performance of PTB-based polymers were made through novel interfacial layer engineering of the OPV device. A conjugated polyelectrolyte was used as an interfacial layer in an inverted device structure, which improved the PCE from 7.4 to 9.2% when using PTB7 and to 10% when using PTB7-Th (Figure 1.1, Polymer 2).[17] A small-molecule zwitterionic non-conjugated electrolyte has also been shown to be an effective charge-injection layer for polymer solar cells, enabling a PCE of over 10% using PTB7-Th polymer.[18]

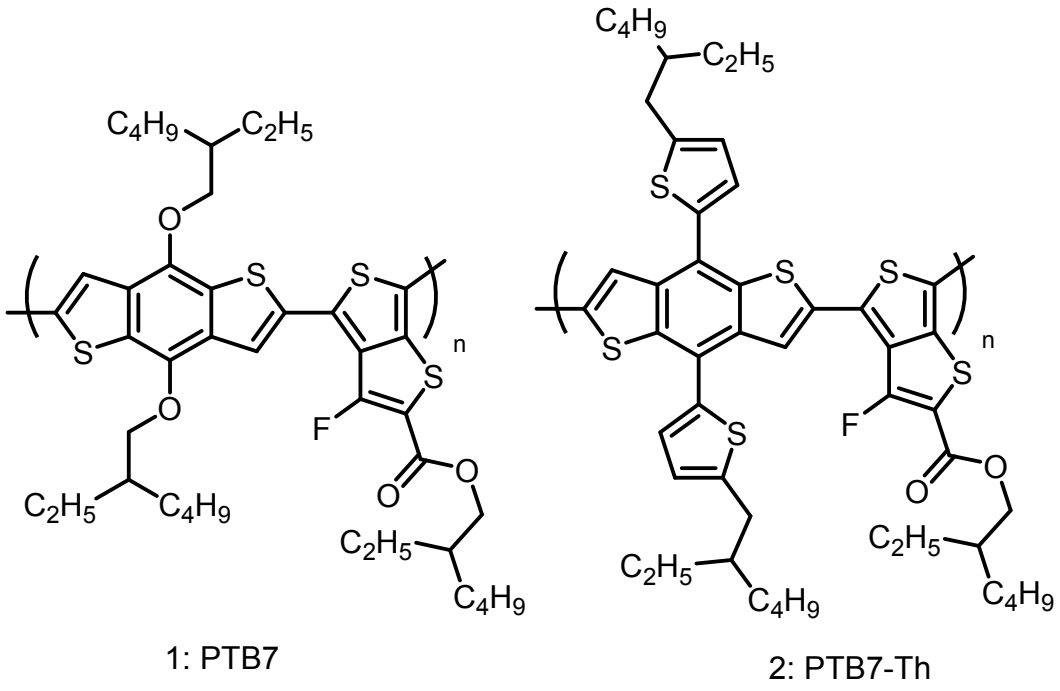

Figure 1.1. Structures of thieno[3,4-b]thiophene based polymers.

1.2.2 *Diketopyrrolopyrrole based polymers*

The first diketopyrrolopyrrole based polymer, poly(diketopyrololpyrrole-terthiophene) or PDPP3T (Figure 1.2, Polymer 3), has a bandgap of 1.31 eV, which allows absorption up to 930 nm.[19] After optimization of molecular mass, a PCE of ~6% was achieved.[20] Combining DPP with thienyl-substituted BDT (BDTT) to form PBDTT–DPP (Figure 1.2, Polymer 4) resulted in a bandgap of 1.44 eV in 2012, and the V_{oc} was higher, indicating that the energy loss was reduced, compared with DPP polymers that had previously been reported. A PCE of ~6.2% was achieved.[21] Modification of PBDTT–DPP with selenium incorporation on the DPP unit to give PBDTT–SeDPP (Figure 1.2, Polymer 5), led to a red-shifted absorption spectrum and PCE of 7.2%.[22] Another notable DPP polymer in recent years includes thieno[3,4-*b*]thiophene-flanked DPP, such as DPPTT-T (Figure 1.2, Polymer 6). DPPTT-T's impressive short circuit current (J_{sc}) of 18.6 mA cm^{-2} was reported in 2013.[23] This material was further studied and incorporated into OPV devices, resulting in an 8.8% PCE solar cell with J_{sc} of 23.5 mA cm^{-2}.[24] DPP-based polymers remain a popular OPV polymer building block.[25]

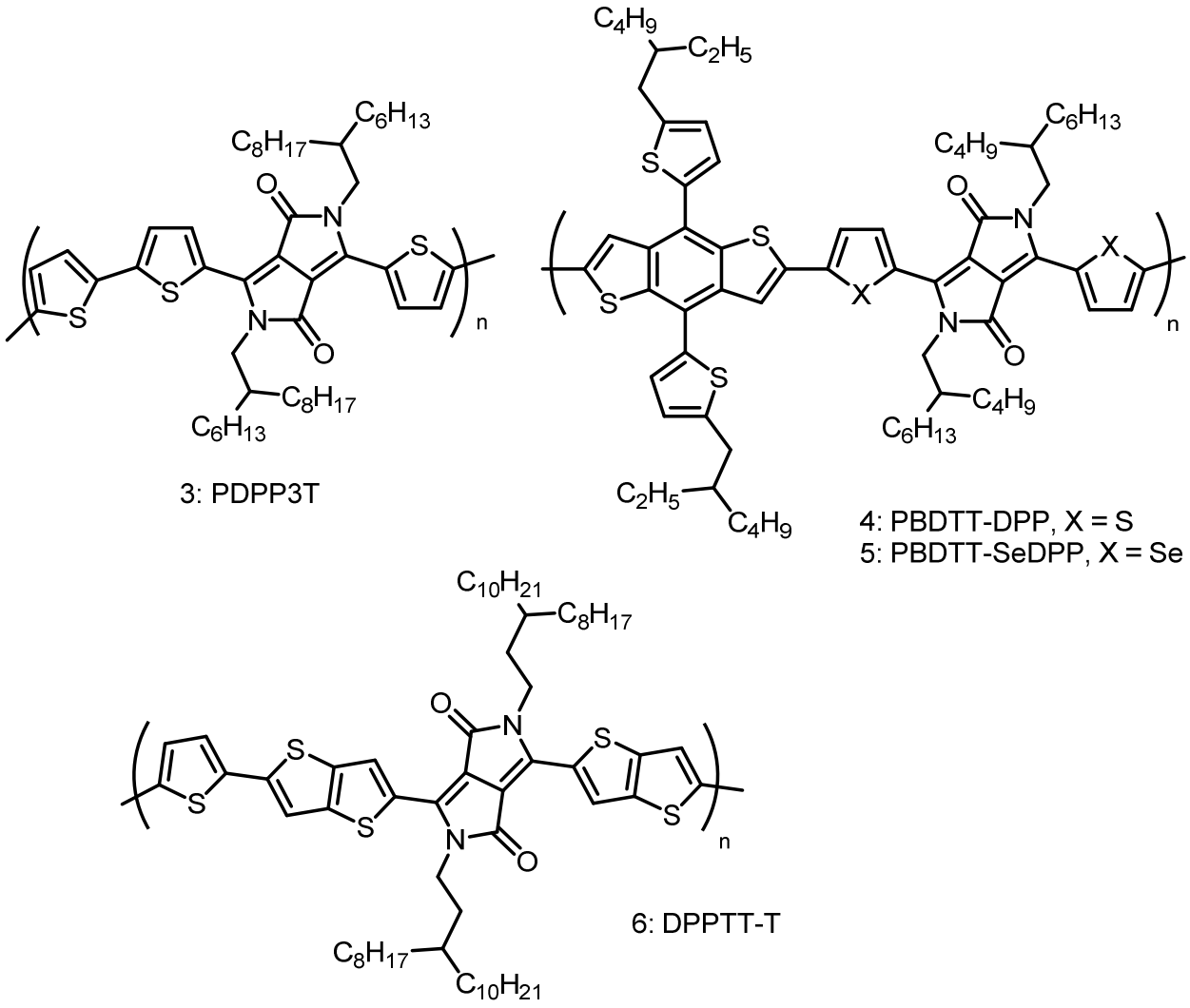

Figure 1.2. Structures of diketopyrrolopyrrole based polymers.

1.2.3 *Benzothiadiazole and difluorobenzothiadiazole based polymers*

Benzothiadiazole (BT) and its derivatives have been widely used as electron-deficient units. PCPDTBT (Figure 1.3, Polymer 7) is a small-bandgap polymer (E_g = 1.4 eV) made by alternating the electron-rich cyclopenta[2,1-*b*;3,4-*b*′]dithiophene (CPDT) and BT units.[26] The PCE of the PCPDTBT-based device was improved from 3 to 5.5% through nanoscale morphology tuning using diiodooctane as an additive.[27]

In 2013, an oxygen-inserted donor, dithieno[3,2-*b*:2′,3′-*d*]pyran (DTP) was introduced as a strong electron donor. When DTP is polymerized with a difluorobenzothiadiazole unit, the polymer obtained, PDTP–DFBT (Figure 1.3, Polymer 8), has a smaller E_g of 1.38 eV and a PCE of 8.0%. The main improvement in the PCE comes from its low-lying HOMO and small bandgap, which result in a large V_{oc} and high J_{sc}. In addition, this polymer presented an external quantum efficiency (EQE) of ~60% in the near-infrared region, which is among the highest reported so far.[28] When combined with a wide bandgap front cell made of poly-(3-hexylthiophene) (P3HT) and indene-C_{60} bisadduct (ICBA), this polymer led to the first tandem polymer solar cell with a PCE above 10%.[29] DFBT was recently polymerized with different thiophene units to form a series of polymers with structures similar to the polymer known as PffBT4T-2OD (Figure 1.3, Polymer 9). Through an interesting high-temperature solution-casting processing method, a PffBT4T-2OD:$PC_{71}BM$ single-junction solar cell showed high PCE and particularly high fill factor of 10.8% and 77%, respectively.[30] Using a similar structure, a high-performing solar cell was processed with a non-halogenated solvent.[31]

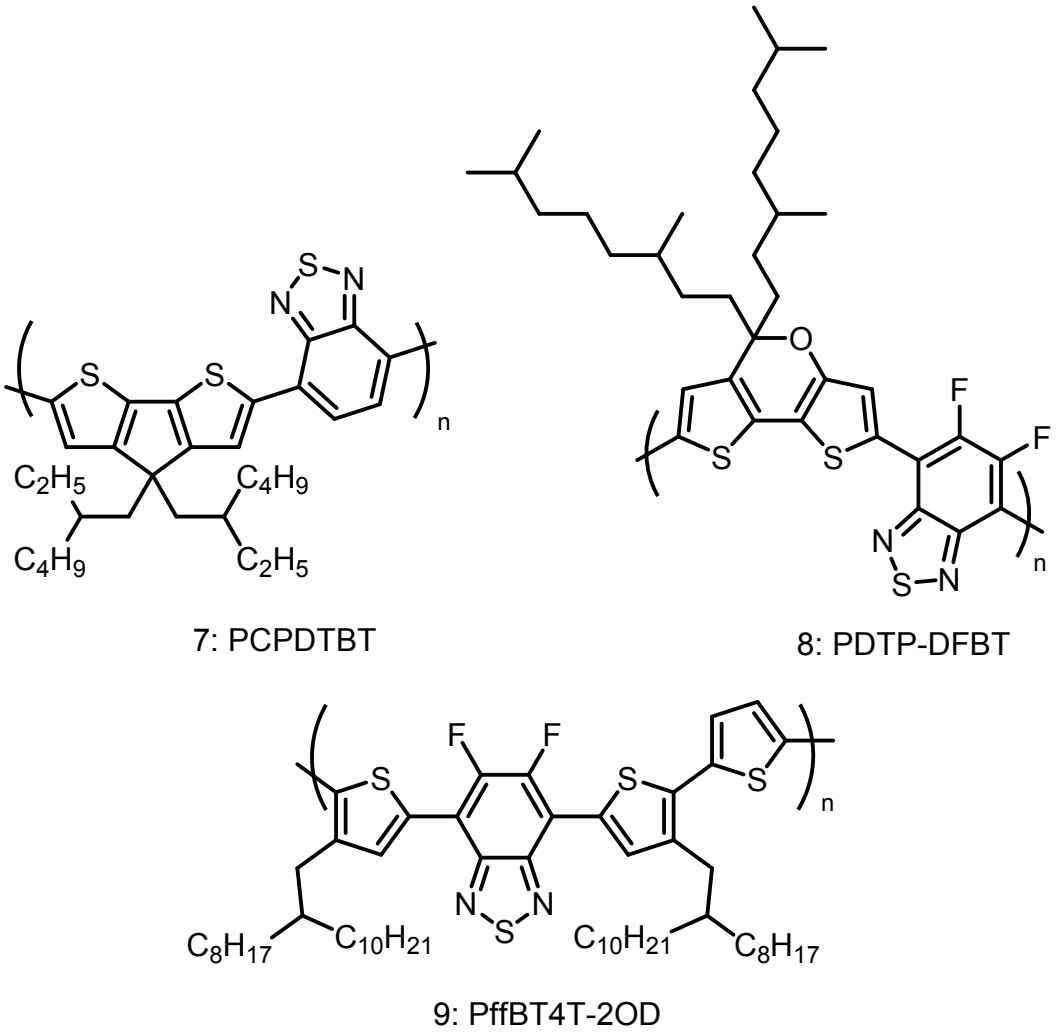

Figure 1.3. Structures of benzothiadiazole based polymers.

The above examples are highlights in a growing field and are in no means a comprehensive list of D-A acceptor polymers. The field continues to grow, and new high performing polymers are developed on a regular basis.

1.3 COST ANALYSIS OF OPV MATERIALS

For organic photovoltaics to become a viable source of renewable energy, the synthesis of organic active-layer materials need to be scaled to thousands of kilograms. Additionally, the ultimate

cost of these materials will need to be low enough to constitute only a small fraction of the cost of the overall solar cell. In 2013, Bulović *et. al.* presented a quantitative analysis, based on published small-scale synthetic procedures, to estimate the materials costs for several promising OPV materials when produced in large quantities.[32] The cost in dollars-per-gram is found to increase linearly with the number of synthetic steps required to produce and purify each organic photoactive compound. The cost-per-Watt ($ per W_p) as a function of power conversion efficiency for an standard OPV structure was found, for a relatively simple molecule requiring only 3 synthetic steps, will contribute a cost of 0.001 to 0.01 $ per W_p, given a solar module PCE of 10%. In comparison, a relatively complicated molecule requiring 14 synthetic steps will contribute costs in the range of 0.075 to 0.48 $ per W_p, suggesting that the commercial viability of an OPV technology may depend on the synthetic accessibility of its active layer materials.

1.4 CONCLUSION

Based on the above study, it can be concluded that there is a need for simplified synthetic methods for D-A polymers. Traditionally D-A polymers rely on many pre-functionalization steps, followed by either Stille or Suzuki cross-coupling based synthetic methods. Many synthetic steps could be eliminated if D-A polymers could be synthesized without the need for functionalization, which is why C-H activation is being explored.

Chapter 2. RECENT DEVELOPMENTS IN C–H ACTIVATION FOR MATERIALS SCIENCE IN THE CENTER FOR SELECTIVE C–H ACTIVATION

*The work in this chapter has previously been published as a review: *Molecules* **2018**, *23*(4), 922; doi:10.3390/molecules23040922*

2.1 INTRODUCTION

Carbon–carbon cross-coupling reactions have proven indispensable for the construction of both small molecule and polymer organic semiconducting materials.[33] Advances in C–H functionalization catalysis now allow for the construction of certain materials directly from their precursor arenes.[34–36] However, in many cases, efficiencies and regioselectivities are not yet sufficiently high, so traditional cross-coupling strategies, in which the regioselectivity of the cross-coupling reaction is predetermined by the synthesis of appropriate organometallic nucleophiles and aryl halide electrophiles, remain important tools for the precise synthesis of novel materials. While many prefunctionalized building blocks are readily obtained by classical reactions (electrophilic aromatic substitution, aryl lithiation, etc.), an increased sophistication in the design of specialized materials, underpinned by a greater understanding of structure–activity relationships and computational predictions, demands a suite of more sophisticated building blocks. C–H functionalization reactions have emerged as a potential path to access novel building blocks that would be difficult to access using traditional chemistry. In addition, C–H functionalization reactions can provide more atom economic syntheses of important materials and building blocks, in many cases using fewer toxic or highly reactive reagents.

In 2012, a materials effort as part of the Center for Selective C–H Functionalization (CCHF) funded by the United States National Science Foundation was tasked with developing C–

H activation chemistry on novel or difficult-to-functionalize intermediates of interest to materials science as well as developing routes for potentially living or living-like C–H activated polymerization. This relatively short feature article mainly reviews the work related to materials chemistry within the NSF-CCHF. As this is a relatively focused review, and since application of C–H functionalization in materials chemistry is a fast-paced and emerging field, the authors regret that it is not possible for us to list all the significant contributions in this field and encourage interested readers to explore other excellent reviews on this topic.[37–39]

2.2 Direct Arylation of Electron-Poor π-Conjugated Small Molecules

π-Conjugated small molecules are used for the fabrication of a variety of organic electronic devices such as dye-sensitized solar cells (DSCs), organic field-effect transistors (OFETs), and organic solar cells (OSCs) and are used extensively in liquid crystalline semiconductors and non-linear optical materials.[40–46] Among the variety of π-conjugated systems reported, electron-donating (D) and electron-accepting units (A) are two key building blocks. By the judicious selection and assembly of varieties of D/A groups along the same backbone, one can make chromophores with desired absorption bandgaps, tailored electron affinity (EA) and ionization energy (IE), and favorable intra/inter-miscibility with surrounding materials.

Electron acceptor building blocks that have relatively high electron affinities and potentially strong intramolecular electron coupling with donor and/or other electron acceptor building blocks are necessary to be able to tune the properties of π-conjugated materials. Properties of specific interest include optical absorption and emission wavelengths, excited state oxidation, reduction potential (e.g., approximate EA), and oxygen stability in electron-

transport materials. Practically, one can design electron-accepting units or molecules through two strategies. (1) Installment of π-withdrawing substituents such as cyano, carbonyls, dicyanovinyl, and the like, on the π-system will typically lower the energy of the lowest unoccupied molecular orbitals (LUMO) and have a smaller impact on the highest occupied molecular orbital (HOMO) levels. This is because the π* energy of the π-withdrawing substituent is often relatively close to that of the LUMO of the unsubstituted conjugated π-system, and the orbitals can thus mix efficiently, leading to stabilization of the LUMO of the electron acceptor building block. (2) Attachment of groups that are predominately inductively electron withdrawing, e.g., perfluoroalkyl groups, can also make a system a stronger electron acceptor. Such substitution indirectly impacts the energy of the π-orbitals by effectively lowering the electron density at the nuclei of the atoms in the π-systems. Therefore, as a consequence, the π-orbitals become less effectively screened and both LUMO and HOMO will tend to be lowered. Similarly, substitution of an atom in a π-system with a more electron-negative atom, such as replacing a carbon of benzene with nitrogen as in pyridine (electronegativity of nitrogen is 3.07 versus 2.50 for carbon), will potentially lower HOMOs and LUMOs.

Manipulation of functional groups on π-electron acceptor units is one of the more challenging topics in traditional organic chemistry. Because of their intrinsically high electron affinity, electrophilic substitutions reactions such as halogenation are difficult to achieve. Additionally, deprotonation to form anions, e.g., to make Stille or Suzuki reagents, often results in nucleophilic addition to the π-electron acceptor and subsequent decomposition. Alternatively, transition metal catalyzed C–H bond functionalization may provide a path to functionalizing strong π-acceptor building blocks without the need for electrophilic substitution

or strongly nucleophilic intermediates. Such metal-mediated reactions, often referred to as direct arylation, have been elegantly applied to electron donor building blocks such as thiophene for small molecule synthesis and even the synthesis of high molecular weight polymers, which requires high starting monomer consumption, regioselectivity, and effectively no deleterious side-reactions.[35,47] Regarding π-electron acceptor substrates, seminal work by Fagnou and coworkers on direct arylation of fluorinated arenes suggested that such reactions occur via a concerted metallation–deprotonation pathway (CMD) on the transition metal that avoids anionic aryl intermediates that are typically highly nucleophilic.[48,49] These reactions in some cases may favor protons in more acidic substrates. This combination of non-nucleophilic intermediates and possible preference for more acidic substrates in certain cases suggested the possibility that such direct arylation might be useful in the functionalization of strong electron acceptors.

Direct C–H bond functionalization reactions are limited by two fundamental challenges: (i) reactivity, the inert nature of most carbon–hydrogen bonds, and (ii) selectivity—the requirement to control regioselectivity in molecules that contain diverse C–H groups. Two main advantages of strong electron acceptors that make them potential candidates for transition metal catalyzed C–H bond functionalization are (i) electronegative elements in electron-acceptor heteroarenes that render certain protons more acidic, which can be abstracted via CMD processes on the metal, and (ii) electron acceptors substituted with carbonyl-related groups (ester, amide, imide, and ketone), which may provide an effective directing group for C–H activation via cyclometallated intermediates. In the following sections, C–H activation of four types of relatively strong electron acceptor building blocks are presented along with their applications in organic electronics.

Benzothiadiazole Derivatives

Derivatives of 2,1,3-benzothiadiazole (BT), especially 5,6-difluorobenzothiadiazole (DFBT) derivatives, have been widely used in organic electronics because of their relatively high electron affinity and planar structures that are favorable to intra- and intermolecular π-coupling.[40] Given the reported harsh conditions for halogenating DFBT or an alternative multistep synthesis, DFBT and potentially other acceptors with higher electron affinity than DFBT were chosen as targets for C–H activated direct arylation.[28,50,51] **Figure 2.1** summarizes a relatively effective coupling strategy that was developed based on the chemistry of Fagnou and coworkers for DFBT and the four electron acceptors: 5,6-dicyanobenzo[*d*][1,2,3]triazole (DCBTz), 6,7-dicyanoquinoxaline (DCQ), 6,7-dinitroquinoxaline (DNQ), and 5,6-dicyano[2,1,3]benzothiadiazole (DCBT).[49] The relative electron affinity of the electron acceptors was determined to be DFBT < DCBTz < DCQ~DNQ < DCBT based on electrochemical and optical measurements.[51] The method proved efficient for a variety of electron-donating and electron-accepting aryl halide substrates and good-to-excellent yields are generally obtained. It should be noted that, under the conditions shown in **Figure 2.1** , C–H activation on the BT alone resulted in multiple arylation at the 5 and 6 positions in addition to the targeted 4 and 7 positions; however, Doucet and co-workers recently reported a phosphine-ligand free mono- and dual C–H activation of 2,1,3-benzothiadiazole in DMA solvent with high-to-moderate yields.[52] Unwanted over-arylation of the products was also seen when coupling the acceptors with 2-bromothiophenes having hydrogen in the 5-positions, which was addressed by the use of 2-bromo-5-(trimethylsilyl)thiophenes. Through proper selection of excess stoichiometry of the acceptor, monoarylated products could be obtained that then could be isolated and arylated again to yield differentially substituted materials with respect to the acceptor moiety such as **1** in **Figure 2.1**. Differentially substituted BT and BTz derivatives have also been obtained by Zhang and

coworkers via selective direct arylation of monobromo BT with aryl iodides or by direct arylation of using an ~3-fold excess of acceptor to the aryl iodide.[53] Zhang and coworkers also reported the direct olefination of BT derivatives with $Pd(OAc)_2$using silver(I) acetate and benzoquinone as co-oxidants to produce a variety of fluorescent compounds.[54]

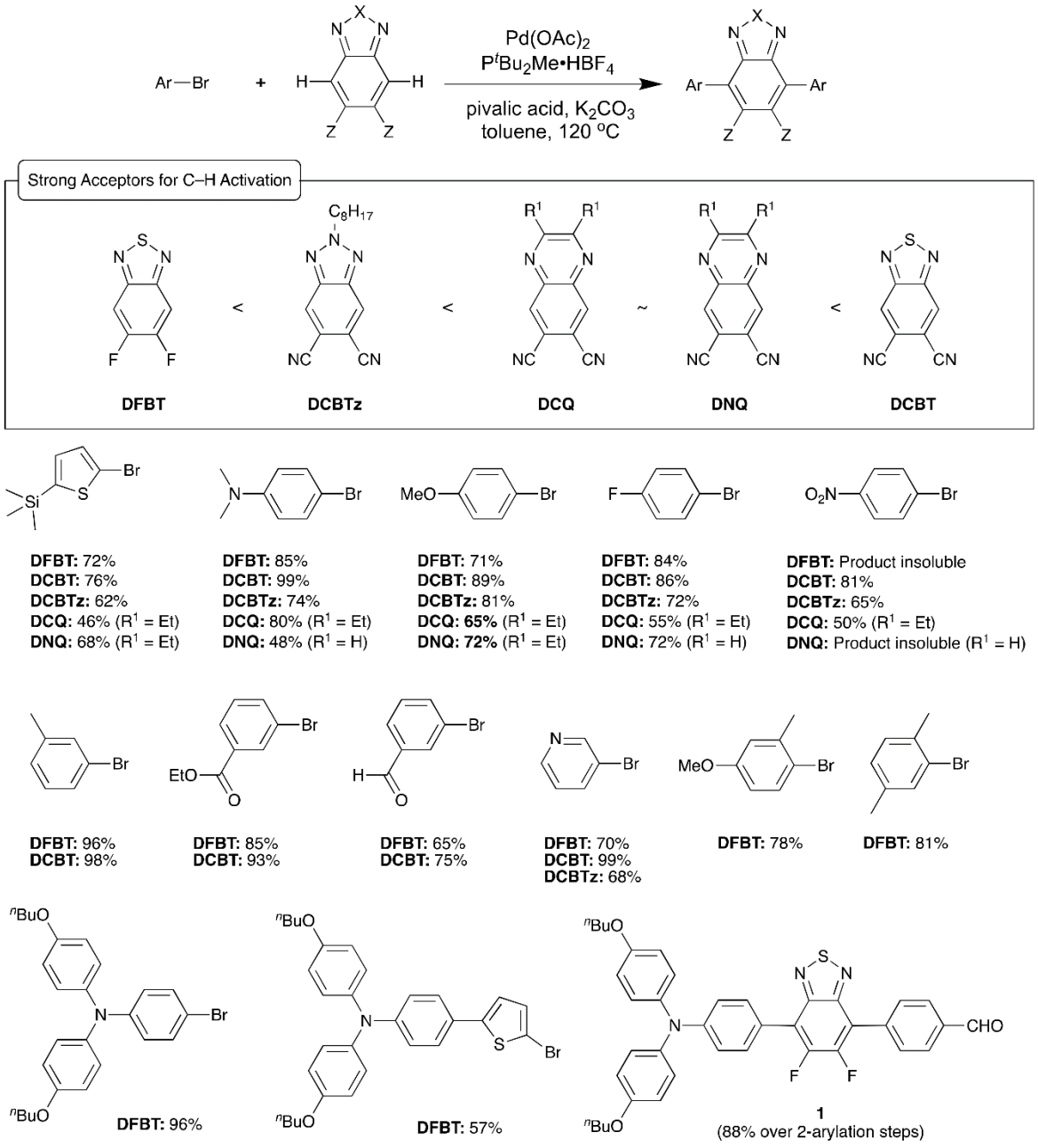

Figure 2.1. Strong electron acceptors for C–H activation with selected aryl halide substrates. Isolated reaction yields for disubstituted acceptor are given. The acceptors appear from left to right in order of increasing estimated electron affinity. In a few cases, the product of the coupling was insoluble in common organic solvents, which are noted.

The conditions summarized in Figure 2.1 have been used in the synthesis of materials **2**–**5** shown in Figure 2.2. Sequential arylations of DFBT were utilized to make a series of D-A-π-A dyes such as **2** in Figure 2.2, incorporating both the donor triarylamine and the π-bridge cyclopentadithiophene (CPDT, as the monoaldehyde), which, after Knoevenagel condensation with cyanoacetic acid, gave chromophores that were incorporated into DSSCs with efficiency up to ~9%.[55,56] Similar conditions have also been used for C–H activation of thienopyrazines such as **3** (Figure 2.2) to yield dicoupled D-A-D chromophores for NIR emitting materials in moderate to high yields.[57] Zhang and coworkers thoroughly optimized C–H coupling conditions between DFBT and dioctylfluorene monomers (21 reaction variations reported) to find similar coupling conditions as shown in **Figure 2.1** for direct arylation polymerization (DArP) to yield **4** (Figure 2.2).[58] Notably, polymerization seemed to stop via reductive debromination and use of BT or 5,6-dialkoxy BT monomers in the polymerization resulted in no significant reaction, suggesting a preference for the electron-accepting substrate DFBT. Under optimized DArP conditions, DFBT Polymer **4** was obtained with an M_n ~41 kg/mol in an 86% yield. Strong electron acceptors were also incorporated into silole-containing polymers such as **5** (Figure 2.2) via C–H activation by Scott and coworkers with a maximum M_n of ~13 kg/mol for coupling with 2,5-di-(4′-bromothienyl)silole derivatives using modified DArP conditions ($Pd(dba)_3$•$CHCl_3$/tris(*o*-methoxyphenyl)phosphine) and with a yield of up to 80%.[59]

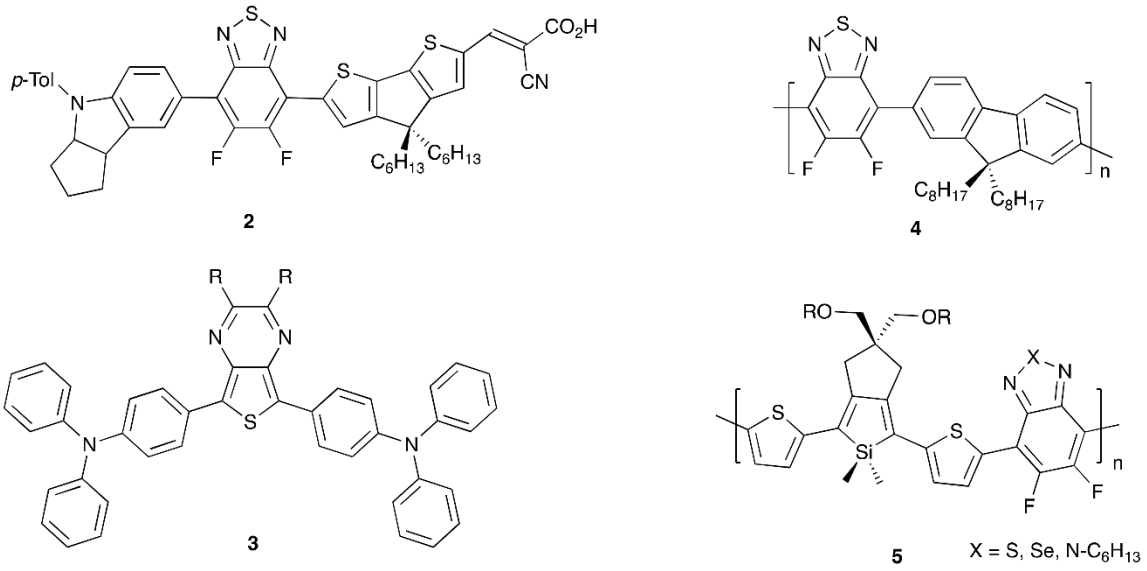

Figure 2.2. π-Conjugated materials synthesized by C–H activated direct arylation similar to that reported in Figure 2.1.

2.3 Earth-Abundant Metal-Initiated Iodination

Other advances in C–H functionalization now allow for the construction of certain intermediates useful in traditional cross coupling reactions directly from the precursor arenes such as Suzuki reagents and aryl silanes via relatively mild catalytic pathways. Such silanes may be used directly in Hiyama coupling or Denmark-Hiyama coupling, or in turn may be converted to aryl halides, Suzuki reagents, Stille reagents, etc.[60–63] In a recent advance, potassium *tert*-butoxide was shown to promote efficient C–H silylation of heteroaromatic systems.[64–66] A similar potassium *tert*-butoxide radial initiation concept has also been applied to the C–H iodination of electron acceptor arenes (Figure 2.3), which are typically resistant to electrophilic aromatic substitution and prone to reduction by organometallic reagents such as alkyl lithium and Grignard reagents that might be employed to deprotonate them.[67] The new C–H iodination reaction proceeds at room temperature, and in many cases a sub-stoichiometric

quantity of potassium *tert*-butoxide is sufficient to provide good reaction yields. In cases where low yields are observed under standard reaction conditions, the use of excess potassium *tert*-butoxide and pentafluorophenyliodide often lead to significant improvements. Highlights noted in Figure 2.3 include the iodination of a range of thiazole derivatives, including a particularly electron-deficient thiazoloperylenediimide, and several benzothiadiazole derivatives. In the case of the mono-fluorobenzothiadiazole, excellent regioselectivity in the iodination reaction is observed to yield the single regioisomer shown.

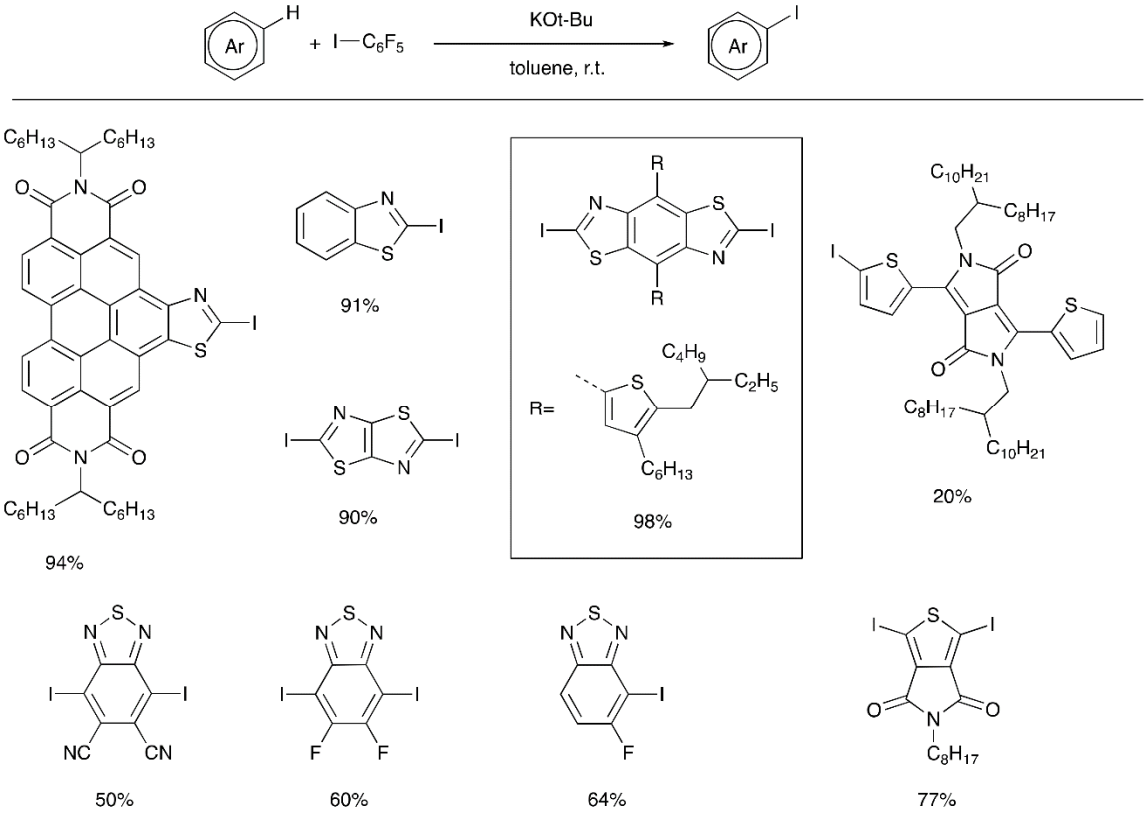

Figure 2.3. Potassium *tert*-butoxide initiated C–H iodination of electron-deficient heteroaromatic compounds.

Subsequent to this discovery of the *tert*-butoxide initiated C–H iodination, additional variations on the reaction conditions, including different initiators, and different halogen sources have been developed.[68] The C–H iodination reaction has been utilized in the synthesis of the non-fullerene acceptor $(TsCDI)_2T$ (Figure 2.4), which demonstrated promising properties as an electron transport material in an organic bulk heterojunction (BHJ) solar cell.[67,69] Subsequently, a direct C–H arylation of the parent PDI-thiazole has been developed enabling a modular synthesis of a number of $(TsCDI)_2$ analogues.[69] Additionally, the application of this reaction in the synthesis of intermediate-sized conjugated donor molecules such as **6** (Figure 2.4), also for application in BHJ solar cells, has been reported.[70]

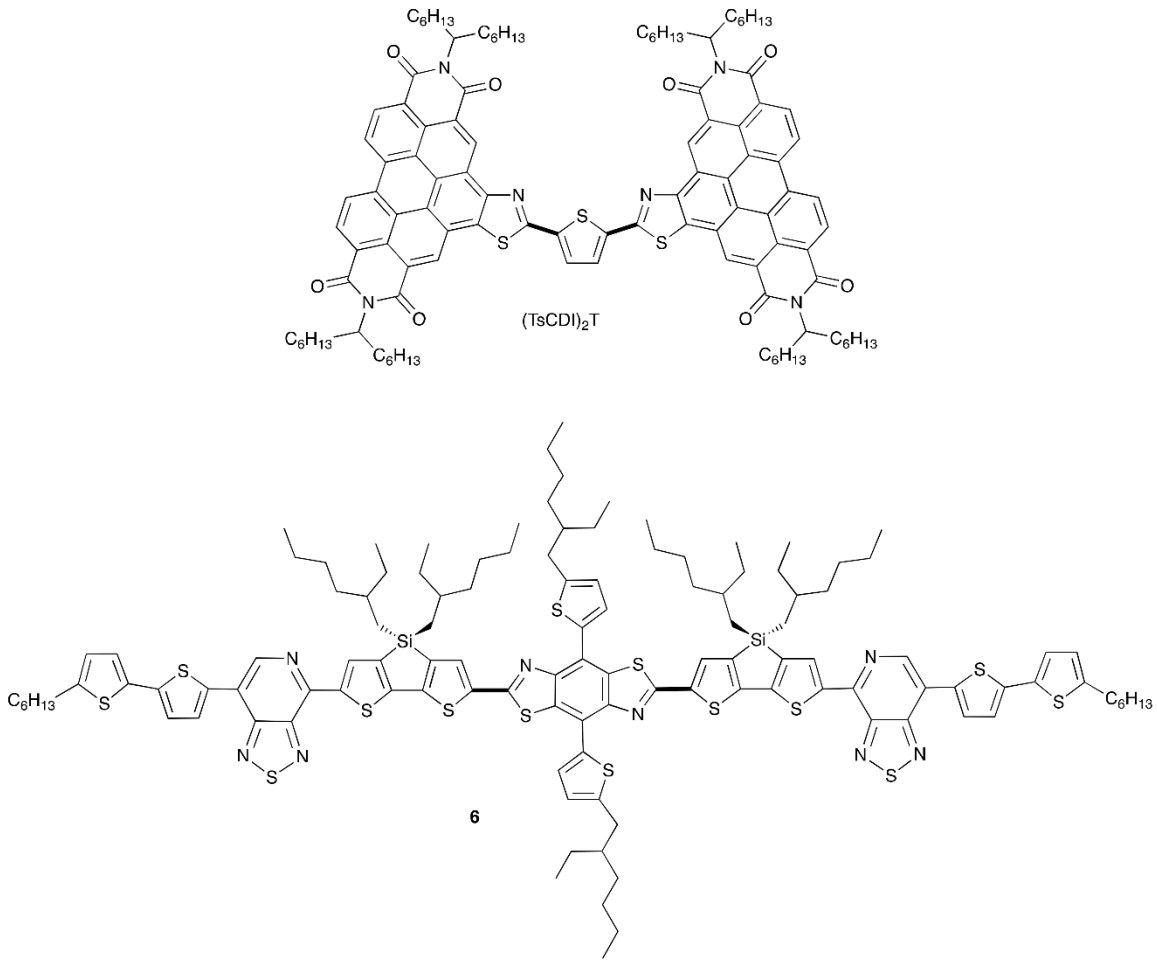

Figure 2.4. Materials constructed using C–H iodination methodology for application in organic photovoltaics.
Bold lines indicate bonds formed by C–H activated direct arylation.

2.4 Toward Living Polymerizations to Synthesize Semiconducting Polymers Using Poly(3-hexylthiophene) as the Model Polymer

Poly(3-hexylthiophene) (P3HT) is one of the most widely used and studied organic electronic polymers partly due to the facile synthesis of specific molecular weight polymers with narrow dispersity (*Đ*). These properties traditionally result from the use of organometallic monomers, synthesized from their respective aryl halide precursors. In 2011, Mori et al.

presented a shortcut to access the organometallic thiophene precursor of P3HT via deprotonation of the thiophene, in which an alkyl magnesium halide and a catalytic amount of an amine base were reacted with 2-chloro-3-hexyl-thiophene to generate the Grignard-monomer prior to polymerization. While this reaction was not enabled by CH-activation, it eliminated the need for a secondary halogenation of the thiophene monomer and used a catalytic amount of base, highlighting the utility to develop more atom-efficient methods to synthesize P3HT.[71] In addition, direct arylation polymerization (DArP) has grown popular for the synthesis of conjugated polymers, but these reactions often lack control over molecular weight and dispersity.[72–74] Therefore, our aim was to design a controlled DArP method with minimal number of steps prior to the actual polymerization, while removing reactive or sensitive reagents such as Grignard compounds. We were attracted to the idea of dual-metal catalysis, where two different metals with orthogonal reactivity are used to selectively activate different steps of the polymerization process.[75,76] Homogeneous gold catalysis has been widely investigated in recent years.[77–79] The attractive features of gold(I) halide compounds are their unlikeliness to undergo oxidative addition with carbon–halogen bonds of aromatic compounds and their ability to insert into electron-deficient aromatic and heteroaromatic C−H bonds, including the C−H activation of bromothiophenes under basic conditions.[80–88] An additional advantage is the ability of gold(I) compounds to undergo transmetalation with palladium(II) complexes, which are commonly utilized to catalyze the C–C coupling of thiophene monomers.[89–93]

To model the concept of dual-metal catalyzed P3HT synthesis (Figure 2.5), a gold and palladium system was explored.[94] First chloro(tri-tert-butylphosphine)gold(I) was utilized to C–H activate and aurylate the 5-position of 2-bromo-3-hexylthiophene, resulting in

Monomer **7** (Figure 2.6). Monomer **7** was then purified and isolated, demonstrating the remarkable stability of the product, especially in comparison to its traditional Grignard counterpart. The purified monomer was polymerized to P3HT using Pd-PEPPSI-iPr as a catalyst (Figure 2.6). The polymerization indicated successful transmetalation and cross-coupling of the aurylated thiophene monomer by the palladium catalyst. In addition, the resulting polymers closely matched the theoretical molecular weights based on the monomer-to-catalyst ratio while also exhibiting narrow dispersities, which correlates with controlled chain-growth polymerization. Upon further investigation, a linear relationship was observed between molecular weight and monomer conversion indicating a single catalyst association to a single polymer chain. The narrow dispersities observed also support a controlled polymerization. The addition of a second equivalent of monomer, after the consumption of the initial monomer, resulted in a predicted doubling of the molecular weight, further supporting the living nature of the polymerization. The good accessibility of **7** via C–H activation and its ability to undergo controlled palladium-catalyzed polymerization open new avenues to explore dual-catalytic DArP with two metals of orthogonal reactivity, without the use of often sensitive organometallic chemicals.

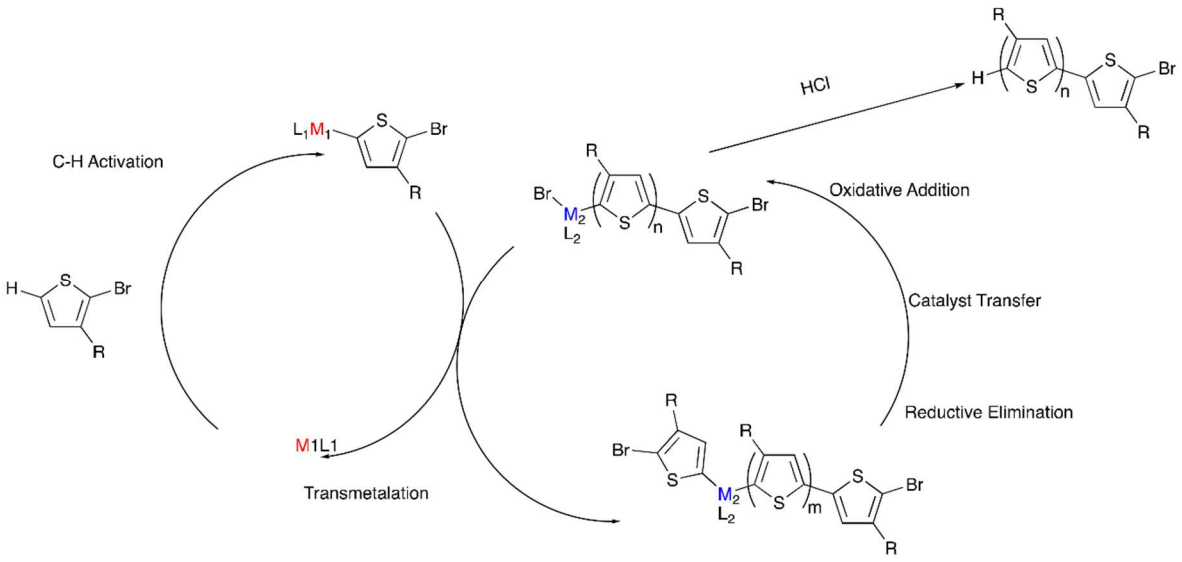

Figure 2.5. Proposed dual-metal catalyzed poly(3-hexylthiophene) (P3HT) synthesis.

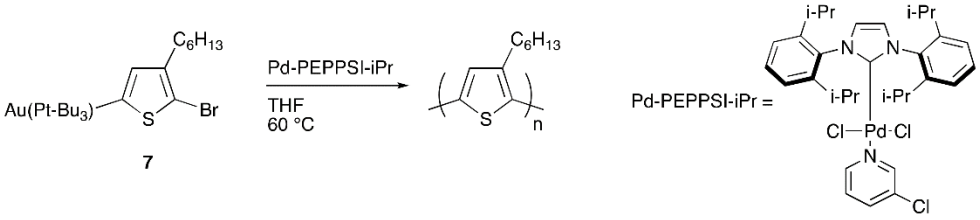

Figure 2.6. Polymerization of aurylated thiophene species.

Moving forward, a dual-catalytic, one-pot polymerization was attempted using the reported gold-palladium conditions; however, polymerization was unfeasible due to hypothesized incompatibilities of the reagents needed for each cycle (Figure 2.5). Silver was explored as another catalyst option, due to promising evidence for its ability to promote C–H activation and to transmetalate with palladium.[95] One-pot reactions (Figure 2.7) resulted in successful polymer synthesis. In the absence of any silver species, polymerization does occur, in which palladium catalyzes both the C–H activation and the C–C coupling. The resulting polymer, however, has low molecular weight and broad dispersity. Incorporation of silver(I)

adamantanoate (AgAd) resulted in increased molecular weight, while the use of silver(I) neodecanoate (AgNDA) resulted in improved regioregularity. Reactions with AgAd provided polymers with narrower dispersities compared to reactions using AgNDA, which resulted in bimodal distributions. Adding 1 equivalent of pyridine with respect to the monomer narrowed the dispersity ($Đ$~1.3–1.4) and yielded unimodality (in the AgNDA system). This was indicative of pyridine's suppression of the number of active species of PEPPSI-iPr, allowing for C–H activation to be primarily silver-mediated, promoting orthogonal reactivity of the two metals, thus yielding chain-growth kinetics. By incorporating both silver for C–H activation and palladium for transmetalation and C–C coupling, chain-growth kinetics with low dispersities (<1.5) were realized, which are not typically observed characteristics of DArP P3HT syntheses.[96–98]

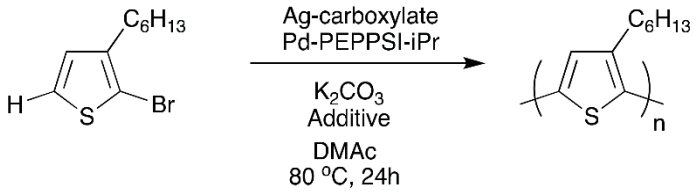

Figure 2.7. One-pot dual-catalytic silver and palladium polymerization.

This is the first reported dual-catalytic silver-palladium system for P3HT synthesis via DArP [69]. The observation of chain-growth, low dispersities, lack of chain transfer, and regioregularity values up to 96% are significant steps toward pursuing a controlled polymerization via DArP. PEPPSI-iPr and silver-carboxylates also possess high chemical stability as opposed to alternative organometallics, which will facilitate less stringent reaction conditions that could have beneficial impacts on ease of synthesis and synthetic scalability. To further this pursuit, understanding the role of active catalytic species and their reaction kinetics could help explain the

current lack of control over the molecular weight. Computational mechanistic insight could also aid in the screening of new ligand, additive, and catalyst moieties.

2.5 Conclusions and Outlook

Although over the last decade a substantial amount of progress has been made by many research groups around the world on the application of C–H activation in materials chemistry, a number of challenges remain and others maybe should be considered. Among those are (1), in aryl halide/thiophene C–H coupling, a higher selectivity for the desired aryl-thiophene bond and less thiophene-thiophene coupling and in particular less coupling of the thiophene in the β-positions, which ideally should effectively be eliminated in favor of high α-thiophene coupling, (2) oxidative C–H/C–H homocoupling, and in particular cross coupling, of both electron acceptors and electron donors in any combination with high selectivity such that excess stoichiometry of one coupling partner is unnecessary and in all cases where oxygen can be used as the terminal oxidant (instead of often large excess of silver(I) salts), (3) post-synthesis diversification of molecules and polymers using other C–H functionalization chemistry that is highly selective for specific sites either on alkyl pendant groups or the aryl core/backbones that would allow probing and optimization of side-chain engineering on morphology and nanoscale intermolecular structure without the need to synthesize a daunting array of intermediates and monomers, (4) use of first row and earth-abundant transition metal catalysts in place of commonly used Pd catalysts, (5) performing the reactions in water, and (6) metal-free synthesis of organic electronic materials. Meeting these challenges, other challenges, and challenges yet to be identified or discovered not only will be critical in providing more sustainable materials development but may also allow researchers to conceive of new materials and research plans with increased breadth that can help define and answer important scientific questions in organic electronic materials.

Chapter 3. EXPLORATION AND DEVELOPMENT OF GOLD- AND SILVER-CATALYZED DEHYDROGENATIVE CROSS-COUPLING TOWARD DONOR-ACCEPTOR POLYMER SYNTHESIS

*sections 3.1-3.4 have been submitted as a manuscript for publication to Polymer Chemistry

3.1 INTRODUCTION

Donor-acceptor (D-A) polymers are a class of semiconducting polymers that have attracted interest in the organic electronics field, due to their favorable properties such as high charge mobility, solution-processability, and low band gaps.[15,99,100] One of the factors that has slowed down commercialization of such polymers in large scale applications is the lack of scalable synthetic methods. In general, D-A polymer syntheses rely on polycondensations that require halogenations and organometallic pre-functionalization steps, such as stannylations for Stille couplings (Fig. 3.1A). Stille couplings are favored for synthesizing D-A polymers because of their high conversion and low catalyst requirements, but the hazardous by-products are undesirable for industrial scale syntheses. Recently there has been growing use of direct heteroarylation polymerization (DHArP) for the synthesis of D-A polymers (Fig. 3.1B).[97,101–103] DHArP involves C-H activation of just one of the aromatic coupling partners while the other is typically halogenated. Thus DHArP reduces the number of monomer pre-functionalization steps required by eliminating the need for specific organometallic functionalization, but still requires halogenation to produce one of the monomers. The use of cross dehydrogenative coupling (CDC), or oxidative CH/CH cross-coupling, in which both coupling partners are selectively C-H activated and then cross-coupled would be far more appealing since neither monomer would have to be pre-functionalized (Fig. 3.1C). Recently, Kanbara *et. al.* demonstrated such a synthetic method with a palladium-catalyzed system in the presence of silver salts to synthesize a copolymer of 2,2′,3,3′,5,5′,6,6′-octafluorobiphenyl and 3,3′-dihexyl-2,2′-bithiophene.[104] Though a successful polymerization of an alternating copolymer was achieved, it remains unclear what the sources of selectivity and the roles of each additive were.

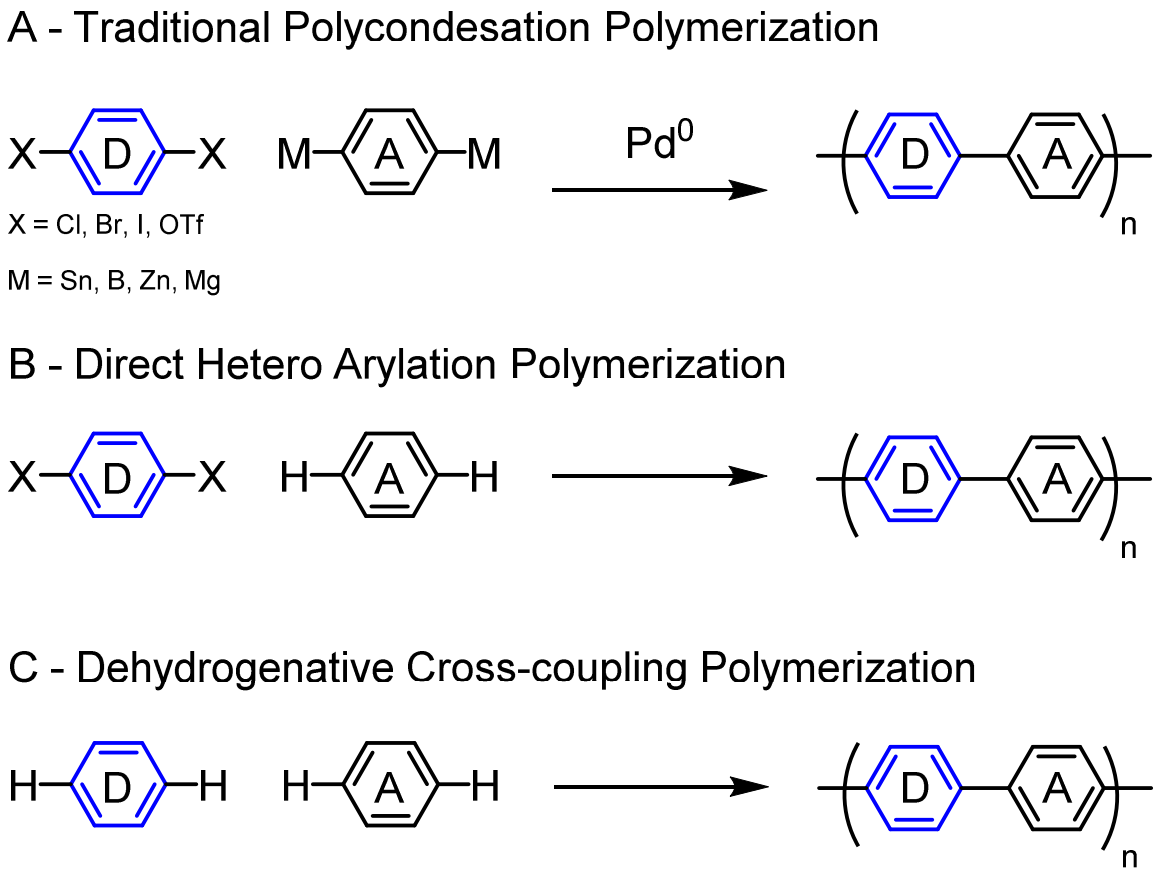

Figure 3.1. Synthetic pathways for donor-acceptor polymers.

Recently, Larossa *et. al.* developed a gold-catalyzed aromatic CDC method for small molecules and observed selectivity in the reactivity of TIPS-protected indoles toward fluorinated benzenes.[105] This methodology achieved direct cross-coupling of simple electron-poor and electron-rich (hetero)arenes with selectivity for the cross-coupled product over the two possible homo-coupled products (Fig 3.2). Additionally, the method did not require the use of directing groups and retained selectivity for the cross-coupling product at close to stoichiometric ratios of the arenes, which has been a challenge for similar Pd-catalyzed systems where typically a large excess of one of the coupling partners is used.[106,107] With seemingly orthogonal reactivity based on substrate electronics, these conditions appeared promising for synthesizing D-A polymers. To this end, we explored the aforementioned method for D-A polymer synthesis, used small molecule model studies to elucidate the factors that contribute to selectivity such as catalyst-driven kinetic

factors and substrate-driven electronic factors, and examined which of these aspects had a more dominant effect in polymer synthesis.

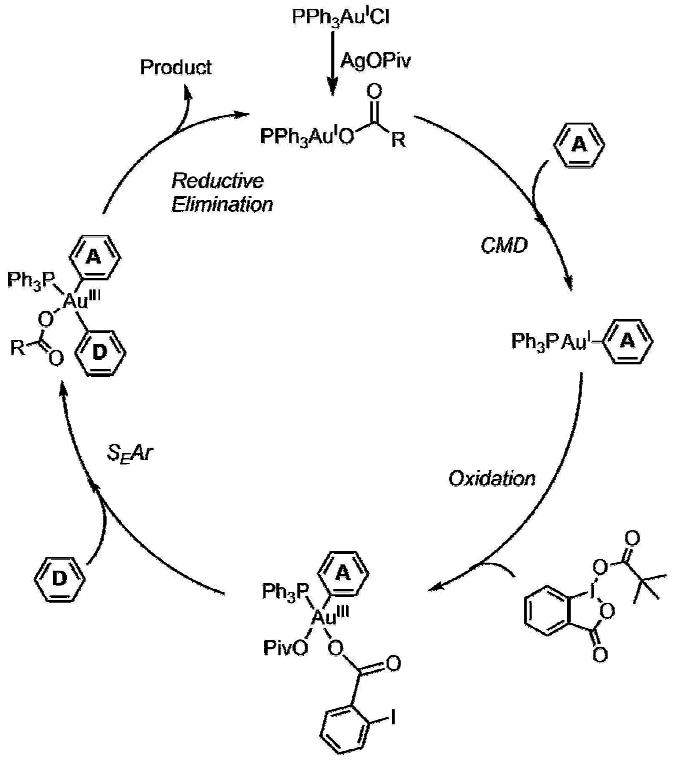

Figure 3.2. Proposed mechanism for Au(I) and Au(III) catalyzed CDC. **A** represents the electron-poor (acceptor) monomer and **D** represents the electron-rich (donor) monomer.

3.2 Results and Discussion

3.2.1 *Preliminary small molecule screening*

The CDC reaction developed by Larossa *et al*. required silver pivalate (AgOPiv), triphenylphosphinegold(I) chloride (PPh_3AuCl), and pivaloyloxy-1,2-benziodoxol-3(1H)-one (PBX). The PBX was used as an oxidant and the gold catalyst was believed to perform the C-H activations and cross-coupling. Specifically, it was presumed that Au(I) activated the electron-poor species and while Au(III) was thought to be for the activation of the electron-rich species (Fig. 3.2).[108] The role of AgOPiv was unclear, as the C-H activation of the electron-poor species did not proceed without AgOPiv but the isolated product of the activation contained a Au(I)-carbon bond, suggesting that Au was responsible for the activation not Ag.

To identify conditions that increased yield of cross-coupled products, a model reaction was performed between 2-methylthiophene (**A**) and pentafluorobenzene (**B**), which were chosen as the electron-rich and electron-poor coupling partners, respectively (Fig. 3.3). Both reagents were selected to prevent any trimer formation, which was observed when the same reactions were run with 1,2,4,5-tetrafluorobenzene as the electron-poor arene. Although trimer formation is promising in the context of polymerization, we elected to block additional reactive sites for this study in order to observe the extent of cross-coupling selectivity between the two coupling partners. These two aromatic compounds were cross-coupled in the presence of AgOPiv, triphenylphosphinegold(I) catalyst (PPh3AuL), and PBX as the oxidant (Table 3.1). Overall, it was clear that the highest cross-coupling occurred with increased AgOPiv loading (Table 3.1, Entries 5 and 10) regardless of the A:B ratio. There was no measurable presence of either homo-coupled product for all entries.

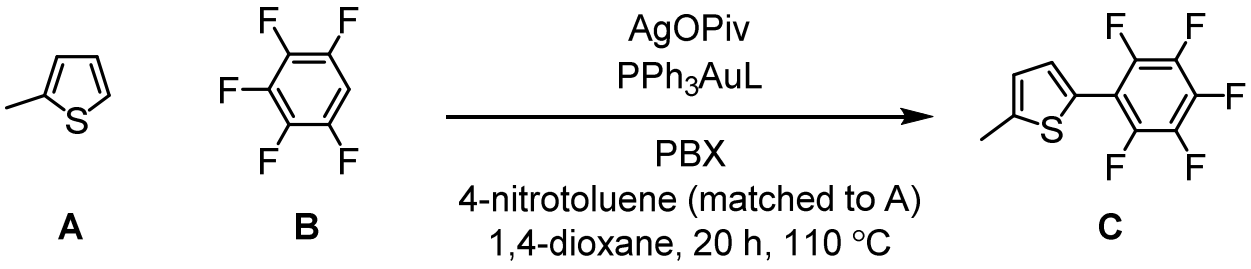

Figure 3.3. Scheme of small molecule dehydrogenative cross-coupling reaction.

Table 3.1. Optimization of small molecule cross-coupling reaction.

Reactions were run on 0.1 mmol scale of A. Reported yields are averages of 3 runs per reaction. The yields were determined by ^{1}H NMR using 4-nitrotoluene as an internal standard, as reported by Larrosa *et. al.*[105] There was no measurable presence of either homo-coupled product.

Entry	Eq. of **A**	Eq of **B**	L	Eq. of AgOPiv	Mol % of Au-catalyst	Eq. of PBX	% yield of C	Rxn Time (h)
1	1	5	Cl	0.35	5	1.5	36±7	20
2	1	5	OAc	0.35	5	1.5	59±5	20
3	1	5	OAc	0.35	5	1.5	82±2	40
4	1	5	OAc	0.7	5	1.5	87±2	20
5	1	5	OAc	1	5	1.5	94±6	20
6	1	1	Cl	0.35	5	1.5	27±8	20
7	1	1	OAc	0.35	5	1.5	20±7	20
8	1	1	OAc	0.35	5	1.5	52±5	40
9	1	1	OAc	0.7	5	1.5	41±9	20
10	1	1	OAc	1	5	1.5	66±12	20
11	1	1	OAc	1	5	1.5	66±3	40

Using these optimized conditions, a polymerization was attempted using 1,2,4,5-tetrafluorobenzene as the electron-poor monomer and 3,3'-dihexyl-2,2'-bithiophene as the electron-rich monomer (Fig 3.4A). The percentage of alternating units in the polymer sequence (% alt) was calculated by integrating the ^{1}H NMR signal of the α-protons on the alkyl chain of the thiophenes (ESI Equation 2). A perfectly alternating polymer would have a % alt of 100 %. The peak of a thiophene positioned between two thiophenes (e.g., AA-AA) appears at 2.53-2.57 ppm, while the α-proton signal of a thiophene located between a fluorinated-benzene and a thiophene (e.g., -BB-AA-) appears at 2.60-2.65 ppm (Figure 3.5). Additionally, number-average molecular weight (M_n) values were determined using end-group analysis via ^{1}H NMR and dispersity ($Đ$) was

determined using size-exclusion chromatography (SEC). The resulting polymer had % alt of 57%, an M_n 0f 5.7 kg/mol, and a $Đ$ *o*f 1.2 after 192 h reaction time. The lower than expected % alt showed that the selectivity observed in the small molecule reaction did not transfer to the polymer synthesis suggesting two possibilities: (i) the terminal protons at the polymer chain-ends would become more electronically similar due to increased conjugation thereby reducing selectivity as the polymer grew; (ii) the previously proposed mechanism as shown in Scheme 1 was not accurate and required further investigation.

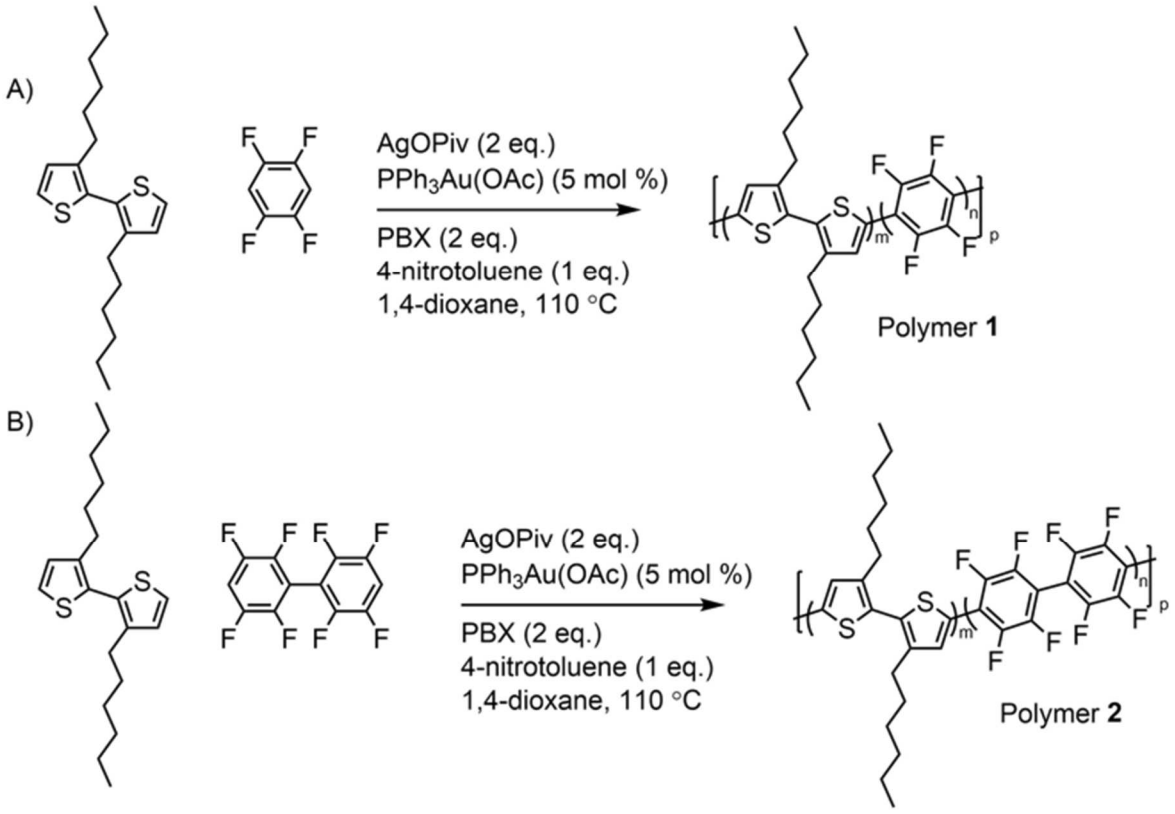

Figure 3.4. Polymerization reaction scheme with 1,2,4,5-tetrafluorobenzene (polymerization 1) and with 2,2',3,3',5,5',6,6'-octafluorobiphenyl (polymerization 2) as the electron-poor monomer. All polymerizations were run on a 1 mmol scale with 1:1 comonomer ratios.

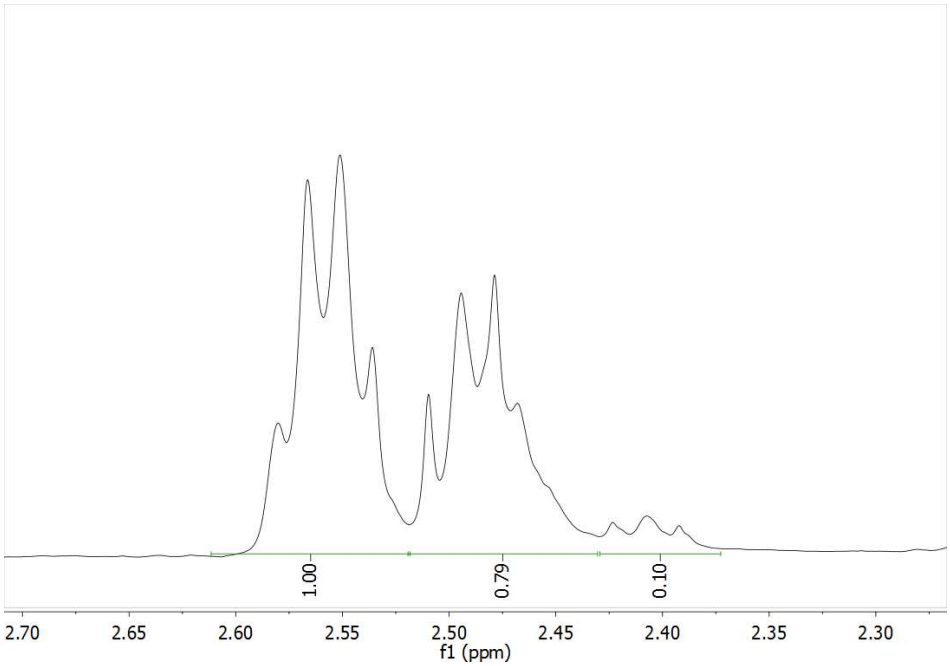

Figure 3.5. Example ^{1}H NMR showing region used for % alt calculation. The ^{1}H NMR corresponds to Polymer 2 in $CDCl_3$ at 192 h timepoint.

3.2.2 *Electronic effect on polymerization*

As already stated, previous work on small molecules had shown that a large component of selectivity came from the difference in the electron density of the starting aryl compounds.[105] In the case of a polymerization, there was a possibility that the terminal protons at the polymer chain-ends would become more electronically similar, regardless of whether they were attached to an electron-rich arene or electron-poor arene, due to increased conjugation thereby reducing selectivity as the polymer grew.

To test if the extended conjugation would negatively affect the selectivity of the terminal proton with polymer growth, polymerizations studies were ran in which the use of 1,2,4,5-tetrafluorobenzene *vs*. 2,2’,3,3’,5,5’,6,6’-octafluorobiphenyl as electron-poor monomers, with 3,3’-dihexyl-2,2’-bithiophene as the electron-rich monomer (Fig. 3.4A and 3.4B) were investigated. It was reasoned that the dihedral angle between the two benzene rings in the octafluorobiphenyl monomer would reduce the effective conjugation length resulting in retaining similar electronic properties of the polymer as the monomeric species[109] allowing us to reduce the potential selectivity issue as the polymer grew. As such, if the selectivity at the polymer chain

ends were indeed problematic, this effect should be observed less when 2,2',3,3',5,5',6,6'-octafluorobiphenyl is used as the monomer (Fig. 3.4B, polymerization 2). Additionally, % alt should decrease with increasing chain length. Aliquots of the polymerization reactions were collected over time and analyzed. As summarized in Table 3.2, it can be seen that the % alt remains at around 55-60% for both systems and does not change significantly as the reaction proceeds. The resulting M_n of polymerizations 1 and 2 were 5.7 kg/mol and 6.5 kg/mol, respectively. The $Đ$ for both polymerizations was determined to be 1.2. The degree of polymerization (DP) of polymerizations 1 and 2 were similar, with values of 21 and 20, respectively. These results suggest that the electronic effect was not a dominating factor as the polymer grew and therefore the substrate-driven selectivity was not the main contributing factor in the % alt of the resultant polymer. Therefore, the mechanism of the polymerization was explored further.

Table 3.2. Results of polymerization reaction comparing 1,2,4,5-tetrafluorobenzene to 2,2',3,3',5,5',6,6'-octafluorobiphenyl as the electron-poor monomer.
Co-monomer ratio loading was 1:1.

Timepoint (h)	% alt for polymerization 1	% alt for polymerization 2
24	61	57
48	61	54
96	61	59
120	58	57
144	69	58
168	54	57
192	57	56

3.2.3 *Cross-coupling mechanism studies*

To elucidate the CDC cross-coupling mechanism, control experiments were run using similar conditions to Fig. 3.3 with AgOPiv, triphenylphosphinegold(I) (PPh_3AuL), and PBX. Of the three reagents listed, uncovering the role of AgOPiv had been the most elusive; the role of silver salts in Pd-catalyzed C-H activation has been the subject of increased studies in recent reports.[95,110,111] It has been proposed that the silver salt could act as an oxidant, as a ligand source, halide scavengers and/or a C-H activating agent.[111] Similarly, for this gold-catalyzed method, AgOPiv

could be playing multiple roles. It was clear from the control experiments that the AgOPiv was not a sufficient oxidant, as the reaction did not proceed without PBX, even in the presence of excess AgOPiv (Table 3.3, Entries 5 and 10). Also, by preforming triphenylphosphinegold(I) acetate ($AuOAcPPh_3$), rather than forming the active gold catalyst *in situ,* as done in previous gold-catalyzed CDC methods using PPh_3AuCl and AgOPiv, we observed that the reaction still required AgOPiv to proceed. Therefore, it was clear that AgOPiv played a larger role than simply as a ligand source or a halide scavenger. There was also an observed decrease in yield with the reduction of the **B** to **A** ratio (Table 3.3, Entries 1, 2, 6, and 7). In combination with the observed increase in yield with increased AgOPiv loading (Table 3.1, Entries 4, 5, 9, and 10), we can conclude that it is likely that both AgOPiv and **B** play a role in the rate-determining step of the reaction.

Table 3.3. Control experiments for dehydrogenative cross-coupling reaction.

Reactions were run on 0.1 mmol scale of A. Reported yields are averages of 3 runs per reaction. The yields were determined by ^1H NMR using 4-nitrotoluene as an internal standard, as reported by Larrosa *et. al.*[105] There was no measurable presence of either homo-coupled product.

Entry	Eq. of **A**	Eq of **B**	L	Eq. of AgOPiv	Mol % of Au-catalyst	Eq. of PBX	% yield of **C**	Rxn Time (h)
1	1	5	Cl	0.35	5	1.5	36±7	20
2	1	5	OAc	0.35	5	1.5	59±5	20
3	1	5	Cl	0	5	1.5	<1	20
4	1	5	OAc	0	5	1.5	<1	20
5	1	5	OAc	0.7	5	0	<1	20
6	1	1	Cl	0.35	5	1.5	27±8	20
7	1	1	OAc	0.35	5	1.5	20±7	20
8	1	1	Cl	0	5	1.5	<1	20
9	1	1	OAc	0	5	1.5	1.1±0.6	20
10	1	1	OAc	0.7	5	0	<1	20

3.2.4 *Deuterium Studies*

As indicated previously, Larrosa *et. al.* had proposed that Au(I) was responsible for activating the electron-poor species and Au(III) was activating the electron-rich species in the presence of PBX and AgOPiv.[85,105] However, since our model studies were suggesting that AgOPiv was playing a bigger role than assumed, deuterium studies were used to elucidate the efficacy of the C-H activating agents. By reacting each of the starting materials (i.e., **A** and **B**) separately with different combinations of additives in the presence of deuterium oxide, the degree of deuteration, and hence C-H activation, could be quantified (Fig. 3.6 and 3.7). Sodium pivalate was used in place of AgOPiv in a control experiment to determine if the pivalate ligand in AgOPiv could deprotonate the starting reagents without the assistance of silver (Table 3.4, Entry 2; Table 3.5, Entry 2). For both **A** and **B**, NaOPiv yielded no C-H activation confirming that pivalate on its own could not deprotonate the starting materials. In the case of tetrafluorobenzene **B**, results in Table 3.4 indicate that AgOPiv itself can act as the C-H activating agent with a deuterium conversion of 23% (Table 3.4, Entry 3), whereas no C-H activation in the presence of Au(I)OAcPPh$_3$ or Au(III) chloride ($AuCl_3$) (Table 3.4, Entry 4-7) was detected going against the previously proposed mechanism in Scheme 1. In the case of 2-methylthiophene (**A**), while some C-H activation occurred in the presence of AgOPiv and AuOAcPPh$_3$, 10% and 4% respectively (Table 3.5, Entries 3 and 7), significantly more activation of 42% was observed in the presence of $AuCl_3$ (Table 3.5, Entry 4), which is in accordance with previously proposed mechanism. Upon the addition of pivalic acid, there was an increase in deuterated product, 69%, showing that the addition of a carboxylate ligand to the gold catalyst increases its ability to C-H activate **B** (Table 3.5, Entry 5). A surprising observation was made in both reactions with **A** and **B** separately, in that the combination of $AuCl_3$ and AgOPiv resulted in reduced C-H activation (Tables 3.4 and 3.5, Entry 6). Futhermore, these reactions also exhibited the formation of silver mirrors on the reaction vessels, indicating a decomposition pathway resulting in the formation of elemental silver. This does not occur in the overall cross-coupling reactions, in which the Au(III) species would have carboxylate anions in place of chloride anions. Therefore, such a decomposition pathway was unique to the highly halogenated Au(III) chloride and does not apply to our overall system. The lack of catalyst decomposition in the overall cross-coupling reaction was confirmed using reaction progress kinetics analysis same excess experiments (ESI Figure 2). Overall, the deuterium studies show that

AgOPiv, not Au(I) as previously thought, activates C-H bond of the electron-poor arene, while the electron-rich species is C-H activated by Au(III).

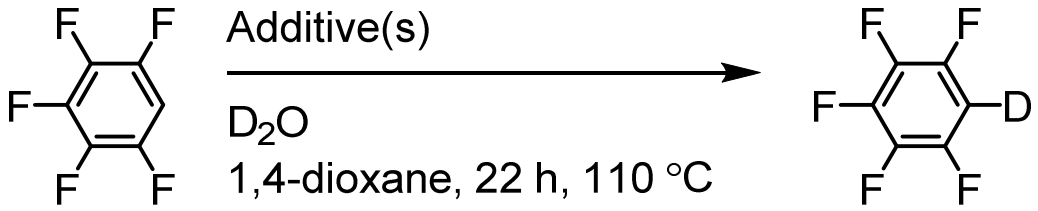

Figure 3.6. Scheme of deuterium study of pentafluorobenzene.

Table 3.4. Deuterium study results of pentafluorobenzene.

Reactions were run on 0.1 mmol scale of A. Reported yields are averages of 3 runs per reaction. The yields were determined by using an internal standard of DMSO-d^6, which was based on similar methods previously reported by Sanford *et. al.*[95]

Entry	Additive	Deuterium Incorporation (%)
1	None	0
2	0.35 eq. NaOPiv	0
3	0.35 eq. AgOPiv	23.1
4	0.005 eq. $AuCl_3$	0
5	0.005 eq. $AuCl_3$, 0.005 eq. PivOH	0
6	0.005 eq. $AuCl_3$, 0.35 eq AgOPiv	1.9
7	0.005 eq. $AuOAcPPh_3$	0
8	0.005 eq. $AuOAcPPh_3$, 0.005 eq. AgOPiv	17.7

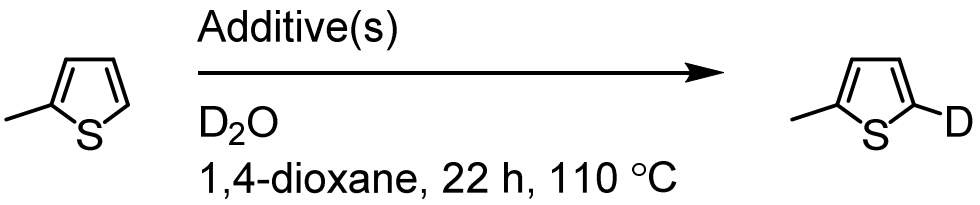

Figure 3.7. Scheme of deuterium study of 2-methylthiophene.

Table 3.5. Deuterium study results of 2-methylthiophene.
Reactions were run on 0.1 mmol scale of A. Reported yields are averages of 3 runs per reaction. The yields were determined by using an internal standard of DMSO-d^6, which was based on similar methods previously reported by Sanford *et. al.*[95]

Entry	Additive	Deuterium Incorporation (%)
1	None	0
2	0.35 eq. NaOPiv	0
3	0.35 eq. AgOPiv	10.0
4	0.005 eq. $AuCl_3$	41.8
5	0.005 eq. $AuCl_3$, 0.005 eq. PivOH	69.3
6	0.005 eq. $AuCl_3$, 0.35 eq. AgOPiv	0
7	0.005 eq. $AuOAcPPh_3$	4.4
8	0.005 eq. $AuOAcPPh_3$, 0.35 eq AgOPiv	6.6

Using the above observations, we propose that the cross-coupling mechanism consists of two overlapping cyclic pathways (Fig 3.8) not just one as shown in Fig. 3.2. The Ag-mediated C-H activation of the fluorinated species appears to be the rate-determining step and is likely slower than the Au-catalyzed C-H activation and the cross-coupling, requiring either increased equivalents of AgOPiv, pentafluorobenzene and/or extended reaction times for higher yield. Also, with the newly elucidated mechanism, we proposed that the rate difference in the C-H activation by Ag vs. Au(III) plays a larger role in the determining how much of each monomer gets incorporated into the final polymer.

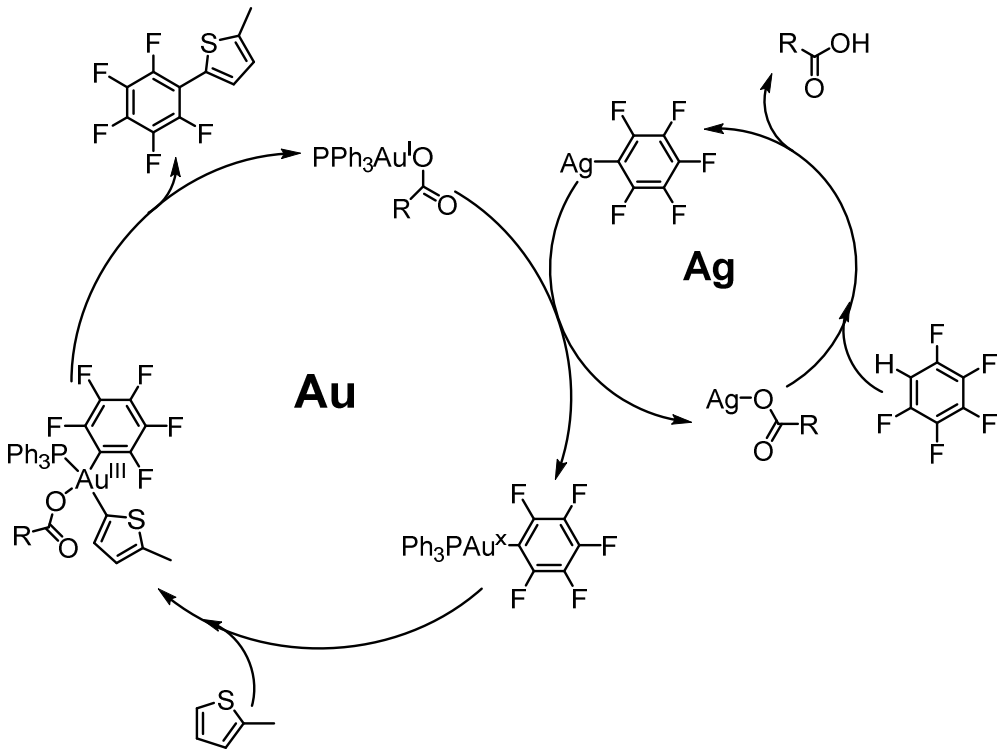

Figure 3.8. Simplified proposed mechanism of gold- and silver-catalyzed dehydrogenative cross-coupling.

3.2.5 *Kinetic effects on polymerization*

The newly proposed mechanism presents a challenge for transitioning the gold- and silver-catalyzed CDC method from a small molecule synthesis to a polymer synthesis. Polymer chain growth in a perfectly alternating manner in a dual cyclic mechanism would require both cycles to turn over in synchrony or for one of the intermediates to be a persistent intermediate.[112] To the extent of our knowledge, there is only one case of polymerization method for a semiconducting polymer that utilizes a dual catalytic mechanism and this was used to synthesize a homopolymer of poly(3-hexylthiophene).[113]

To test the effect of kinetic mismatch between the two cycles on the resulting polymer, we designed an experiment to have a pseudo-excess of the fluorinated species since we had observed that increased pentafluorobenzene loading resulted in higher yields of the cross-coupled product for the small molecule reactions. We used the same conditions of Scheme 3, but the 3,3'-dihexyl-2,2'-bithiophene was added to the polymerization mixture at different rates using a syringe pump.

For these studies, 2,2',3,3',5,5',6,6'-octafluorobiphenyl was used as the electron-poor monomer. As the rate of addition of the thiophene mixture was decreased, the % alt of the resulting polymer increased (Table 3.6). This indicated that higher selectivity for degree of alternation was achievable by slow bithiophene addition compared to the previous reaction conditions that start with both monomers in one-pot. In addition, with longer injections times, dispersity decreased from 1.3 to 1.1. The reduced yields with reduced rate of addition may be indicative of reduced incorporation of monomer overall. Changing the rate of 3,3'-dihexyl-2,2'-bithiophene addition to the reaction mixture is clearly impactful on the resulting polymer, indicating that the kinetics of reaction is crucial for both selectivity for alternating monomer incorporation as well as overall reactivity. This new understanding of the impact of kinetics due to the dual-catalytic cycle provides a potential for controlling the ratio of A:B monomer incorporation. For example, by changing the offset of the two catalytic cycles, there could be an easy control for selecting between an $(\text{-AB-})_n$ polymer as compared to an $(\text{-AAB-})_n$ polymer. This would be a useful tool because D-A polymers have been altered with different numbers of thiophene spacers to change their electronic and mechanical properties.[114]

Table **3.6**. Slow addition of thiophene studies.

Injection time (h)	Post-injection reaction time (h)	% alternating	NMR M_n (kg/mol)	$Đ$	Yield (%)
0	120	45	2.6	1.3	63
12	120	46	2.7	1.2	13
48	120	65	3.1	1.1	2
72	120	79	5.6	1.1	1

3.3 CONCLUSIONS

In conclusion, we applied the gold- and silver-catalyzed CDC method to D-A polymer synthesis. It was determined that the overall change in electron-density in the growing polymer did not impact the overall selectivity for cross-coupling vs homo-coupling. In the small molecule model studies, we have elucidated the roles of the various reagents in the small molecule studies of the gold- and silver-catalyzed CDC. It was found that AgOPiv was essential for the reaction to proceed, even without the need for a halogen acceptor, a ligand source, or an oxidant, as it activated the C-H

bond of electron-poor coupling partner. Screening experiments also indicated that the silver-catalyzed C-H activation of electron-poor species was most likely the rate-limiting step. By combining our findings, we were able to propose a novel mechanism with two cycles working in tandem, which added a kinetic challenge for the polymerization. In changing the addition rate of the thiophene species, we could observe that an increase in selectivity for cross-coupling. This suggests that the kinetic mismatch of the catalysts may be exploited for synthesizing D-A polymers of specific ratios. The originally proposed monometallic Au(I)/Au(III)-catalyzed mechanism may have appeared ideal for an $(\text{-AB-})_n$ alternating copolymer synthesis, but ultimately these studies show that the multimetallic nature of the mechanism may provide a new tool for controlling the ratio of A:B incorporated into final polymer using kinetics potentially leading towards the facile synthesis of sequence-controlled polymers.

3.4 EXPERIMENTAL

3.4.1 *General procedures and materials*

All manipulation of air- and/or moisture-sensitive compounds were carried out using standard Schlenk and glovebox techniques under a dry nitrogen atmosphere. Anhydrous 1,4-dioxane, 1,2,4,5-tetrafluorobenzene, 2-methylthiophene, 4-nitrotoluene, chloro(triphenylphosphine)gold(I), 2,2',3,3',5,5',6,6'-octafluorobiphenyl, 3,3'-dihexyl-2,2'-bithiophene, gold(III) chloride, deuterium oxide, sodium trimethylacetate hydrate, and pivalic acid were used as purchased. Pivaloyloxy-1,2-benziodoxol-3(1H)-one (PBX),[105] silver pivalate (AgOPiv),[115] and acetate(triphenylphosphine)gold(I) ($Au(OAc)PPh_3$)[116] were synthesized using previously reported methods.

3.4.2 *Cross-coupling studies*

A 4mL amber vial and an acid-washed stir bar were oven dried overnight. Gold(I) catalyst, silver pivalate, 4-nitrotoluene (1 eq. to 2-methylthiophene), and PBX were added to the previously

mentioned vial and sealed with a septa cap. Vial was evacuated and refilled with nitrogen three times. Under nitrogen pressure, anhydrous 1,4-dioxane (0.2 M relative to 2-methylthiophene), 1,2,4,5-tetrafluorobenzene, and 2-methylthiophene were injected into the reaction flasks in succession. The reactions were heated at 110 °C overnight. The resulting mixtures were passed through a celite plug using hexanes, washed with 1 M HCl, followed by 1 M NaOH, and then the organic layer was dried using anhydrous Na_2SO_4. The remaining solvent was removed under reduced pressure. The resulting mixtures were analyzed by NMR.

3.4.3 *Deuterium studies*

A 4mL amber vial and an acid-washed stir bar were oven dried overnight. Varied combinations of additives were added and then the vial was evacuated and refilled with nitrogen three times. Under nitrogen pressure, 0.5 mL of anhydrous 1,4-dioxane, 0.1 mmol of 2-methylthiophene or 1,2,4,5-tetrafluorobenzene, and 0.5 mmol of deuterium oxide were injected into the reaction flasks in succession. The reactions were heated at 110 °C overnight. The resulting mixtures were passed through a celite plug. 10 μL of d_6-acetone were added. The mixture was analyzed using ^2H NMR, by comparing the deuterated aryl peak against the d_6-acetone peak.

3.4.4 *Dehydrogenative Cross-coupling Polymerization*

A 20 mL amber vial and an acid-washed stir bar were oven dried overnight. Gold(I) catalyst (5 mol %), silver pivalate (2 eq.), 4-nitrotoluene (1 eq.), and PBX (2 eq.) were added to the previously mentioned vial and sealed with a septa cap. Vial was evacuated and refilled with nitrogen three times. Under nitrogen pressure, anhydrous 1,4-dioxane (0.2 M relative to 3,3'-dihexyl-2,2'-bithiophene), 2,2',3,3',5,5',6,6'-octafluorobiphenyl (1 mmol), and 3,3'-dihexyl-2,2'-bithiophene (1 mmol) were injected into the reaction flasks in succession. The reactions were

heated at 110 ° C. The reaction was quenched with 1 M HCl. The resulting mixture was washed with saturated EDTA solution, and then precipitated into excess MeOH. Then the resulting polymer was Soxhlet extracted with MeOH, then collected in chloroform. The remaining solvent was removed under reduced pressure. The resulting mixtures were analyzed by NMR, GPC, MALDI.

3.4.5 *Slow Thiophene Addition Dehydrogenative Cross-coupling Polymerization*

A 20 mL amber vial and an acid-washed stir bar were oven dried overnight. Gold(I) catalyst (5 mol %), silver pivalate (2 eq.), 4-nitrotoluene (1 eq.), and PBX (2 eq.) were added to the previously mentioned vial and sealed with a septa cap. Vial was evacuated and refilled with nitrogen three times. Under nitrogen pressure, anhydrous 2 mL of 1,4-dioxane and 2,2',3,3',5,5',6,6'-octafluorobiphenyl (1 mmol) were injected into the reaction flasks in succession. The reactions were heated at 110 ° C. 1 mmol of 3,3'-dihexyl-2,2'-bithiophene in 3 mL of anhydrous 1,4-dioxane was added dropwise, using a syringe pump. After complete injection of the mixture, the reaction continued for 120 h. The reaction was quenched with 1 M HCl. The resulting mixture was washed with saturated EDTA solution, and then precipitated into excess MeOH. Then the resulting polymer was Soxhlet extracted with MeOH, then collected in chloroform. The remaining solvent was removed under reduced pressure. The resulting mixtures were analyzed by NMR, GPC, MALDI.

3.5 FUTURE WORK

3.5.1 *Explore one-pot polymerization kinetic controls*

As observed in Table 3.6, 0 h injection time, decent yields and dispersities were observed. This shows us that it would be worth improving on such conditions. The variables to change would be initial concentrations of AgOPiv and stir speeds. These would be to increase the Ag-catalyzed

cycle. Since the AgOPiv is insoluble, resulting in a heterogeneous reaction mixture, the stirring can play a large role in reactivity. If necessary, it may be worth exploring different carboxylate ligands on the silver-catalyst.

3.5.2 *Target specific sequences of monomer incorporation*

By combining the kinetic control with the dual-catalytic mechanism, this method presents an opportunity to select between specific sequence incorporation. (i.e. $(\text{-DA-})_n$ vs. $(\text{-DDA-})_n$)
If the above optimization presents kinetic control over the reaction using the concentration of AgOPiv, this can be exploited for selectively and reproducibly synthesizing sequence specific polymers. For this, it would be require synthesizing model polymers of specific sequences using traditional polycondensation methods, for comparison standards for analysis. Specifically, these model polymers could be used to compare the UV-Vis of the different sequence polymers. Additionally the ligand screening from the previous study should also be beneficial for controlling the sequence as well.

3.5.3 *Combine findings for 95% alternation D-A polymer*

The traditional polycondensation methods and DHArp methods usually result in about 5-10% homocoupling defects in their resulting polymers, therefore we can set our goals to synthesize similar polymers using a CDC method.
To achieve this, it would be worth elucidating the rates of each step of the overall mechanism, to decipher how large of a kinetic offset there is between the two C-H activation steps.

BIBLIOGRAPHY

[1] J. L. Brédas, *J. Chem. Phys.* **1985**, *82*, 3808–3811.
[2] G. Brocks, A. Tol, *J. Phys. Chem.* **1996**, *100*, 1838–1846.
[3] Y.-J. Cheng, S.-H. Yang, C.-S. Hsu, *Chem. Rev.* **2009**, *109*, 5868–5923.
[4] G. L. Gibson, T. M. McCormick, D. S. Seferos, *J. Am. Chem. Soc.* **2012**, *134*, 539–547.
[5] Y.-J. Cheng, T.-Y. Luh, *J. Organomet. Chem.* **2004**, *689*, 4137–4148.
[6] J. D. Yuen, F. Wudl, *Energy Environ. Sci.* **2013**, *6*, 392–406.
[7] D. Letian, Y. Jingbi, H. Ziruo, X. Zheng, L. Gang, S. R. A., Y. Yang, *Adv. Mater.* **2013**, *25*, 6642–6671.
[8] L. Dou, Y. Liu, Z. Hong, G. Li, Y. Yang, *Chem. Rev.* **2015**, *115*, 12633–12665.
[9] Y. Liang, Y. Wu, D. Feng, S.-T. Tsai, H.-J. Son, G. Li, L. Yu, *J. Am. Chem. Soc.* **2009**, *131*, 56–57.
[10] L. Yongye, X. Zheng, X. Jiangbin, T. Szu-Ting, W. Yue, L. Gang, R. Claire, Y. Luping, *Adv. Mater.* **2010**, *22*, E135–E138.
[11] J. Hou, M.-H. Park, S. Zhang, Y. Yao, L.-M. Chen, J.-H. Li, Y. Yang, *Macromolecules* **2008**, *41*, 6012–6018.
[12] Y. Liang, D. Feng, Y. Wu, S.-T. Tsai, G. Li, C. Ray, L. Yu, *J. Am. Chem. Soc.* **2009**, *131*, 7792–7799.
[13] H.-Y. Chen, J. Hou, S. Zhang, Y. Liang, G. Yang, Y. Yang, L. Yu, Y. Wu, G. Li, *Nat. Photonics* **2009**, *3*, 649.
[14] L. Luyao, Y. Luping, *Adv. Mater.* **2014**, *26*, 4413–4430.
[15] J. Hou, H.-Y. Chen, S. Zhang, R. I. Chen, Y. Yang, Y. Wu, G. Li, *J. Am. Chem. Soc.* **2009**, *131*, 15586–15587.
[16] L. Sih-Hao, J. Hong-Jyun, C. Yu-Shan, C. Show-An, *Adv. Mater.* **2013**, *25*, 4766–4771.
[17] Z. He, B. Xiao, F. Liu, H. Wu, Y. Yang, S. Xiao, C. Wang, T. P. Russell, Y. Cao, *Nat. Photonics* **2015**, *9*, 174.
[18] X. Ouyang, R. Peng, L. Ai, X. Zhang, Z. Ge, *Nat. Photonics* **2015**, *9*, 520.
[19] J. C. Bijleveld, A. P. Zoombelt, S. G. J. Mathijssen, M. M. Wienk, M. Turbiez, D. M. de Leeuw, R. A. J. Janssen, *J. Am. Chem. Soc.* **2009**, *131*, 16616–16617.
[20] H. K. H., H. G. H. L., G. V. S., W. M. M., J. R. A. J., *Angew. Chemie Int. Ed.* **2013**, *52*, 8341–8344.
[21] L. Dou, J. You, J. Yang, C.-C. Chen, Y. He, S. Murase, T. Moriarty, K. Emery, G. Li, Y. Yang, *Nat. Photonics* **2012**, *6*, 180.
[22] D. Letian, C. Wei-Hsuan, G. Jing, C. Chun-Chao, Y. Jingbi, Y. Yang, *Adv. Mater.* **2012**, *25*, 825–831.
[23] I. Meager, R. S. Ashraf, S. Mollinger, B. C. Schroeder, H. Bronstein, D. Beatrup, M. S. Vezie, T. Kirchartz, A. Salleo, J. Nelson, et al., *J. Am. Chem. Soc.* **2013**, *135*, 11537–11540.
[24] R. S. Ashraf, I. Meager, M. Nikolka, M. Kirkus, M. Planells, B. C. Schroeder, S. Holliday, M. Hurhangee, C. B. Nielsen, H. Sirringhaus, et al., *J. Am. Chem. Soc.* **2015**, *137*, 1314–1321.
[25] K. H. Hendriks, W. Li, M. M. Wienk, R. A. J. Janssen, *J. Am. Chem. Soc.* **2014**, *136*, 12130–12136.
[26] M. D., S. M., M. M., Z. Z., W. D., G. R., B. C., *Adv. Mater.* **2006**, *18*, 2884–2889.
[27] J. Peet, J. Y. Kim, N. E. Coates, W. L. Ma, D. Moses, A. J. Heeger, G. C. Bazan, *Nat.*

Mater. **2007**, *6*, 497.
[28] L. Dou, C.-C. Chen, K. Yoshimura, K. Ohya, W.-H. Chang, J. Gao, Y. Liu, E. Richard, Y. Yang, *Macromolecules* **2013**, *46*, 3384–3390.
[29] J. You, L. Dou, K. Yoshimura, T. Kato, K. Ohya, T. Moriarty, K. Emery, C.-C. Chen, J. Gao, G. Li, et al., *Nat. Commun.* **2013**, *4*, 1446.
[30] Y. Liu, J. Zhao, Z. Li, C. Mu, W. Ma, H. Hu, K. Jiang, H. Lin, H. Ade, H. Yan, *Nat. Commun.* **2014**, *5*, 5293.
[31] J. Zhao, Y. Li, G. Yang, K. Jiang, H. Lin, H. Ade, W. Ma, H. Yan, *Nat. Energy* **2016**, *1*, 15027.
[32] T. P. Osedach, T. L. Andrew, V. Bulović, *Energy Environ. Sci.* **2013**, *6*, 711–718.
[33] M. Giuseppe, C. C. V., B. Francesco, B. Gabriele, P. Andrea, P. Riccardo, F. G. M., *European J. Org. Chem.* **2014**, *2014*, 6583–6614.
[34] S. Kowalski, S. Allard, K. Zilberberg, T. Riedl, U. Scherf, *Prog. Polym. Sci.* **2013**, *38*, 1805–1814.
[35] D. J. Schipper, K. Fagnou, *Chem. Mater.* **2011**, *23*, 1594–1600.
[36] D. Alberico, M. E. Scott, M. Lautens, *Chem. Rev.* **2007**, *107*, 174–238.
[37] H. Bohra, M. Wang, *J. Mater. Chem. A* **2017**, *5*, 11550–11571.
[38] J.-R. Pouliot, F. Grenier, J. T. Blaskovits, S. Beaupré, M. Leclerc, *Chem. Rev.* **2016**, *116*, 14225–14274.
[39] S.-L. Suraru, J. A. Lee, C. K. Luscombe, *ACS Macro Lett.* **2016**, *5*, 724–729.
[40] X. Guo, M. Baumgarten, K. Müllen, *Prog. Polym. Sci.* **2013**, *38*, 1832–1908.
[41] A. Hagfeldt, G. Boschloo, L. Sun, L. Kloo, H. Pettersson, *Chem. Rev.* **2010**, *110*, 6595–6663.
[42] H. Klauk, *Chem. Soc. Rev.* **2010**, *39*, 2643–2666.
[43] H. Zhou, L. Yang, W. You, *Macromolecules* **2012**, *45*, 607–632.
[44] Y. Lin, Y. Li, X. Zhan, *Chem. Soc. Rev.* **2012**, *41*, 4245–4272.
[45] H. Iino, J. Hanna, *Polym. J.* **2016**, *49*, 23.
[46] L. R. Dalton, P. A. Sullivan, D. H. Bale, *Chem. Rev.* **2010**, *110*, 25–55.
[47] L. G. Mercier, M. Leclerc, *Acc. Chem. Res.* **2013**, *46*, 1597–1605.
[48] D. Lapointe, K. Fagnou, *Chem. Lett.* **2010**, *39*, 1118–1126.
[49] M. Lafrance, C. N. Rowley, T. K. Woo, K. Fagnou, *J. Am. Chem. Soc.* **2006**, *128*, 8754–8756.
[50] Y. Zhang, S.-C. Chien, K.-S. Chen, H.-L. Yip, Y. Sun, J. A. Davies, F.-C. Chen, A. K.-Y. Jen, *Chem. Commun.* **2011**, *47*, 11026–11028.
[51] J. Zhang, T. C. Parker, W. Chen, L. Williams, V. N. Khrustalev, E. V Jucov, S. Barlow, T. V Timofeeva, S. R. Marder, *J. Org. Chem.* **2016**, *81*, 360–370.
[52] I. Idris, T. Tannoux, F. Derridj, V. Dorcet, J. Boixel, V. Guerchais, J.-F. Soulé, H. Doucet, *J. Mater. Chem. C* **2018**, *6*, 1731–1737.
[53] C.-Y. He, C.-Z. Wu, F.-L. Qing, X. Zhang, *J. Org. Chem.* **2014**, *79*, 1712–1718.
[54] X. Yu-Lan, Z. Bo, H. Chun-Yang, Z. Xingang, *Chem. – A Eur. J.* **2014**, *20*, 4532–4536.
[55] X. Kang, J. Zhang, D. O'Neil, A. J. Rojas, W. Chen, P. Szymanski, S. R. Marder, M. A. El-Sayed, *Chem. Mater.* **2014**, *26*, 4486–4493.
[56] X. Kang, J. Zhang, A. J. Rojas, D. O'Neil, P. Szymanski, S. R. Marder, M. A. El-Sayed, *J. Mater. Chem. A* **2014**, *2*, 11229–11234.
[57] L. E. McNamara, N. Liyanage, A. Peddapuram, J. S. Murphy, J. H. Delcamp, N. I. Hammer, *J. Org. Chem.* **2016**, *81*, 32–42.

[58] Z. Xiaojie, G. Yao, L. Sida, S. Xincui, G. Yanhou, W. Fosong, *J. Polym. Sci. Part A Polym. Chem.* **2014**, *52*, 2367–2374.
[59] C. N. Scott, M. D. Bisen, D. M. Stemer, S. McKinnon, C. K. Luscombe, *Macromolecules* **2017**, *50*, 4623–4628.
[60] I. A. I. Mkhalid, J. H. Barnard, T. B. Marder, J. M. Murphy, J. F. Hartwig, *Chem. Rev.* **2010**, *110*, 890–931.
[61] C. Cheng, J. F. Hartwig, *Chem. Rev.* **2015**, *115*, 8946–8975.
[62] Y. Hatanaka, T. Hiyama, *J. Org. Chem.* **1988**, *53*, 918–920.
[63] S. E. Denmark, C. S. Regens, *Acc. Chem. Res.* **2008**, *41*, 1486–1499.
[64] A. A. Toutov, W.-B. Liu, K. N. Betz, A. Fedorov, B. M. Stoltz, R. H. Grubbs, *Nature* **2015**, *518*, 80.
[65] W.-B. Liu, D. P. Schuman, Y.-F. Yang, A. A. Toutov, Y. Liang, H. F. T. Klare, N. Nesnas, M. Oestreich, D. G. Blackmond, S. C. Virgil, et al., *J. Am. Chem. Soc.* **2017**, *139*, 6867–6879.
[66] S. Banerjee, Y.-F. Yang, I. D. Jenkins, Y. Liang, A. A. Toutov, W.-B. Liu, D. P. Schuman, R. H. Grubbs, B. M. Stoltz, E. H. Krenske, et al., *J. Am. Chem. Soc.* **2017**, *139*, 6880–6887.
[67] Q. Shi, S. Zhang, J. Zhang, V. F. Oswald, A. Amassian, S. R. Marder, S. B. Blakey, *J. Am. Chem. Soc.* **2016**, *138*, 3946–3949.
[68] X. Liu, X. Zhao, F. Liang, B. Ren, *Org. Biomol. Chem.* **2018**, *16*, 886–890.
[69] Q. Shi, E. S. Andreansky, S. R. Marder, S. B. Blakey, *J. Org. Chem.* **2017**, *82*, 10139–10148.
[70] S. Zhang, J. Zhang, M. Abdelsamie, Q. Shi, Y. Zhang, T. C. Parker, E. V Jucov, T. V Timofeeva, A. Amassian, G. C. Bazan, et al., *Chem. Mater.* **2017**, *29*, 7880–7887.
[71] S. Tamba, K. Shono, A. Sugie, A. Mori, *J. Am. Chem. Soc.* **2011**, *133*, 9700–9703.
[72] A. Facchetti, L. Vaccaro, A. Marrocchi, *Angew. Chemie Int. Ed.* **2012**, *51*, 3520–3523.
[73] K. Okamoto, J. Zhang, J. B. Housekeeper, S. R. Marder, C. K. Luscombe, *Macromolecules* **2013**, *46*, 8059–8078.
[74] Y. Segawa, T. Maekawa, K. Itami, *Angew. Chemie Int. Ed.* **2015**, *54*, 66–81.
[75] M. H. Pérez-Temprano, J. A. Casares, P. Espinet, *Chem. – A Eur. J.* **2012**, *18*, 1864–1884.
[76] T. L. Lohr, T. J. Marks, *Nat. Chem.* **2015**, *7*, 477.
[77] A. S. K. Hashmi, G. J. Hutchings, *Angew. Chemie Int. Ed.* **2006**, *45*, 7896–7936.
[78] A. Fürstner, P. W. Davies, *Angew. Chemie Int. Ed.* **2007**, *46*, 3410–3449.
[79] H. A. Wegner, M. Auzias, *Angew. Chemie Int. Ed.* **2011**, *50*, 8236–8247.
[80] T. Lauterbach, M. Livendahl, A. Rosellón, P. Espinet, A. M. Echavarren, *Org. Lett.* **2010**, *12*, 3006–3009.
[81] M. Livendahl, C. Goehry, F. Maseras, A. M. Echavarren, *Chem. Commun.* **2014**, *50*, 1533–1536.
[82] M. Joost, A. Zeineddine, L. Estévez, S. Mallet−Ladeira, K. Miqueu, A. Amgoune, D. Bourissou, *J. Am. Chem. Soc.* **2014**, *136*, 14654–14657.
[83] J. Guenther, S. Mallet-Ladeira, L. Estevez, K. Miqueu, A. Amgoune, D. Bourissou, *J. Am. Chem. Soc.* **2014**, *136*, 1778–1781.
[84] X. C. Cambeiro, T. C. Boorman, P. Lu, I. Larrosa, *Angew. Chemie Int. Ed.* **2013**, *52*, 1781–1784.
[85] T. C. Boorman, I. Larrosa, *Chem. Soc. Rev.* **2011**, *40*, 1910–1925.
[86] I. I. F. Boogaerts, S. P. Nolan, *J. Am. Chem. Soc.* **2010**, *132*, 8858–8859.

[87] S. Gaillard, C. S. J. Cazin, S. P. Nolan, *Acc. Chem. Res.* **2012**, *45*, 778–787.
[88] N. Ahlsten, G. J. P. Perry, X. C. Cambeiro, T. C. Boorman, I. Larrosa, *Catal. Sci. Technol.* **2013**, *3*, 2892–2897.
[89] M. M. Hansmann, M. Pernpointner, R. Döpp, A. S. K. Hashmi, *Chem. – A Eur. J.* **2013**, *19*, 15290–15303.
[90] A. S. K. Hashmi, R. Döpp, C. Lothschütz, M. Rudolph, D. Riedel, F. Rominger, *Adv. Synth. Catal.* **2010**, *352*, 1307–1314.
[91] J. delPozo, J. A. Casares, P. Espinet, *Chem. Commun.* **2013**, *49*, 7246–7248.
[92] Y. Shi, K. E. Roth, S. D. Ramgren, S. A. Blum, *J. Am. Chem. Soc.* **2009**, *131*, 18022–18023.
[93] M. H. Pérez-Temprano, J. A. Casares, Á. R. de Lera, R. Álvarez, P. Espinet, *Angew. Chemie Int. Ed.* **2012**, *51*, 4917–4920.
[94] S.-L. Suraru, J. A. Lee, C. K. Luscombe, *ACS Macro Lett.* **2016**, *5*, 533–536.
[95] M. D. Lotz, N. M. Camasso, A. J. Canty, M. S. Sanford, *Organometallics* **2017**, *36*, 165–171.
[96] Q. Wang, R. Takita, Y. Kikuzaki, F. Ozawa, *J. Am. Chem. Soc.* **2010**, *132*, 11420–11421.
[97] Y.-Y. Lai, T.-C. Tung, W.-W. Liang, Y.-J. Cheng, *Macromolecules* **2015**, *48*, 2978–2988.
[98] A. E. Rudenko, B. C. Thompson, *Macromolecules* **2015**, *48*, 569–575.
[99] K. Müllen, W. Pisula, *J. Am. Chem. Soc.* **2015**, *137*, 9503–9505.
[100] S. Holliday, Y. Li, C. K. Luscombe, *Prog. Polym. Sci.* **2017**, *70*, 34–51.
[101] Y. Hendsbee, A.D.; Li, *Molecules* **2018**, *23*, 1255.
[102] T. Bura, J. T. Blaskovits, M. Leclerc, *J. Am. Chem. Soc.* **2016**, *138*, 10056–10071.
[103] C. Roy, T. Bura, S. Beaupré, M.-A. Légaré, J.-P. Sun, I. G. Hill, M. Leclerc, *Macromolecules* **2017**, *50*, 4658–4667.
[104] H. Aoki, H. Saito, Y. Shimoyama, J. Kuwabara, T. Yasuda, T. Kanbara, *ACS Macro Lett.* **2018**, *7*, 90–94.
[105] X. C. Cambeiro, N. Ahlsten, I. Larrosa, *J. Am. Chem. Soc.* **2015**, *137*, 15636–15639.
[106] D. R. Stuart, K. Fagnou, *Science (80-.).* **2007**, *316*, 1172 LP-1175.
[107] C.-Y. He, Q.-Q. Min, X. Zhang, *Organometallics* **2012**, *31*, 1335–1340.
[108] P. Lu, T. C. Boorman, A. M. Z. Slawin, I. Larrosa, *J. Am. Chem. Soc.* **2010**, *132*, 5580–5581.
[109] F. Grein, *J. Phys. Chem. A* **2002**, *106*, 3823–3827.
[110] D. Whitaker, J. Burés, I. Larrosa, *J. Am. Chem. Soc.* **2016**, *138*, 8384–8387.
[111] K. L. Bay, Y.-F. Yang, K. N. Houk, *J. Organomet. Chem.* **2018**, *864*, 19–25.
[112] L. K. G. Ackerman, M. M. Lovell, D. J. Weix, *Nature* **2015**, *524*, 454.
[113] J. A. Lee, C. K. Luscombe, *ACS Macro Lett.* **2018**, *7*, 767–771.
[114] P. Sista, J. Hao, S. Elkassih, E. E. Sheina, M. C. Biewer, B. G. Janesko, M. C. Stefan, *J. Polym. Sci. Part A Polym. Chem.* **2011**, *49*, 4172–4179.
[115] D. A. Edwards, R. M. Harker, M. F. Mahon, K. C. Molloy, *Inorganica Chim. Acta* **2002**, *328*, 134–146.
[116] P. García-Domínguez, C. Nevado, *J. Am. Chem. Soc.* **2016**, *138*, 3266–3269.
[117] B. D. G., *Angew. Chemie Int. Ed.* **2005**, *44*, 4302–4320.
[118] R. S. Loewe, P. C. Ewbank, J. Liu, L. Zhai, R. D. McCullough, *Macromolecules* **2001**, *34*, 4324–4333.
[119] A. Yokoyama, R. Miyakoshi, T. Yokozawa, *Macromolecules* **2004**, *37*, 1169–1171.
[120] H. Sirringhaus, P. J. Brown, R. H. Friend, M. M. Nielsen, K. Bechgaard, B. M. W.

Langeveld-Voss, A. J. H. Spiering, R. A. J. Janssen, E. W. Meijer, P. Herwig, et al., *Nature* **1999**, *401*, 685–688.
[121] J. Y. Kim, K. Lee, N. E. Coates, D. Moses, T.-Q. Nguyen, M. Dante, A. J. Heeger, *Sci.* **2007**, *317*, 222–225.
[122] I. Osaka, R. D. McCullough, *Acc. Chem. Res.* **2008**, *41*, 1202–1214.
[123] A. Salleo, R. J. Kline, D. M. DeLongchamp, M. L. Chabinyc, *Adv. Mater.* **2010**, *22*, 3812–3838.
[124] M. He, F. Qiu, Z. Lin, *J. Mater. Chem.* **2011**, *21*, 17039–17048.
[125] K. Okamoto, C. K. Luscombe, *Polym. Chem.* **2011**, *2*, 2424–2434.
[126] A. Marrocchi, D. Lanari, A. Facchetti, L. Vaccaro, *Energy Environ. Sci.* **2012**, *5*, 8457–8474.
[127] Q. Zhang, T. P. Russell, T. Emrick, *Chem. Mater.* **2007**, *19*, 3712–3716.
[128] B. P. Khanal, E. R. Zubarev, *Angew. Chem. Int. Ed. Engl.* **2009**, *48*, 6888–91.
[129] M. He, F. Qiu, Z. Lin, *J. Phys. Chem. Lett.* **2013**, *4*, 1788–1796.
[130] R. A. Krüger, T. J. Gordon, T. Baumgartner, T. C. Sutherland, *ACS Appl. Mater. Interfaces* **2011**, *3*, 2031–2041.
[131] A. L. Briseno, T. W. Holcombe, A. I. Boukai, E. C. Garnett, S. W. Shelton, J. J. M. Fréchet, P. Yang, *Nano Lett.* **2010**, *10*, 334–340.
[132] H. A. Bronstein, C. K. Luscombe, *J. Am. Chem. Soc.* **2009**, *131*, 12894–12895.
[133] A. Smeets, K. Van den Bergh, J. De Winter, P. Gerbaux, T. Verbiest, G. Koeckelberghs, *Macromolecules* **2009**, *42*, 7638–7641.
[134] V. Senkovskyy, M. Sommer, R. Tkachov, H. Komber, W. T. S. Huck, A. Kiriy, *Macromolecules* **2010**, *43*, 10157–10161.
[135] N. Doubina, A. Ho, A. K.-Y. Jen, C. K. Luscombe, *Macromolecules* **2009**, *42*, 7670–7677.
[136] V. Senkovskyy, R. Tkachov, T. Beryozkina, H. Komber, U. Oertel, M. Horecha, V. Bocharova, M. Stamm, S. A. Gevorgyan, F. C. Krebs, et al., *J. Am. Chem. Soc.* **2009**, *131*, 16445–16453.
[137] N. Doubina, S. A. Paniagua, A. V Soldatova, A. K. Y. Jen, S. R. Marder, C. K. Luscombe, *Macromolecules* **2011**, *44*, 512–520.
[138] A. Smeets, P. Willot, J. De Winter, P. Gerbaux, T. Verbiest, G. Koeckelberghs, *Macromolecules* **2011**, *44*, 6017–6025.
[139] M. Jeffries-El, G. Sauvé, R. D. McCullough, *Macromolecules* **2005**, *38*, 10346–10352.
[140] B. M. W. Langeveld-Voss, R. A. J. Janssen, A. J. H. Spiering, J. L. J. van Dongen, E. C. Vonk, H. A. Claessens, *Chem. Commun.* **2000**, 81–82.
[141] M. Jeffries-EL, G. Sauvé, R. D. McCullough, *Adv. Mater.* **2004**, *16*, 1017–1019.
[142] W. M. Kochemba, S. M. Kilbey, D. L. Pickel, *J. Polym. Sci. Part A Polym. Chem.* **2012**, *50*, 2762–2769.
[143] R. H. Lohwasser, M. Thelakkat, *Macromolecules* **2011**, *44*, 3388–3397.
[144] W. M. Kochemba, D. L. Pickel, B. G. Sumpter, J. Chen, S. M. Kilbey, *Chem. Mater.* **2012**, *24*, 4459–4467.
[145] Z. Mao, K. Vakhshouri, C. Jaye, D. A. Fischer, R. Fernando, D. M. DeLongchamp, E. D. Gomez, G. Sauvé, *Macromolecules* **2013**, *46*, 103–112.
[146] J. Liu, R. D. McCullough, *Macromolecules* **2002**, *35*, 9882–9889.
[147] R. H. Lohwasser, M. Thelakkat, *Macromolecules* **2010**, *43*, 7611–7616.
[148] L. Zhang, K. Hashimoto, K. Tajima, *Polym J* **2012**, *44*, 1145–1148.

[149] J. C. Love, L. A. Estroff, J. K. Kriebel, R. G. Nuzzo, G. M. Whitesides, *Chem. Rev.* **2005**, *105*, 1103–1169.
[150] K. Okamoto, C. K. Luscombe, *Chem. Commun.* **2014**, *50*, 5310–5312.

APPENDIX A

Chapter 4. SUPPLEMENTARY INFORMATION FOR CHAPTER 3

4.1 GENERAL PROCEDURES

All manipulation of air- and/or moisture-sensitive compounds were carried out using standard Schlenk and glovebox techniques under a dry nitrogen atmosphere. Anhydrous 1,4-dioxane, 1,2,4,5-tetrafluorobenzene, 2-methylthiophene, 4-nitrotoluene, chloro(triphenylphosphine)gold(I), 2,2',3,3',5,5',6,6'-octafluorobiphenyl, 3,3'-dihexyl-2,2'-bithiophene, gold(III) chloride, deuterium oxide, sodium trimethylacetate hydrate, and pivalic acid were used as purchased. Pivaloyloxy-1,2-benziodoxol-3(1H)-one (PBX),[105] silver pivalate (AgOPiv),[115] and acetate(triphenylphosphine)gold(I) ($Au(OAc)PPh_3$)[116] were synthesized using previously reported methods. ^1H NMR and ^2H NMR spectra were collected on a Bruker AV 500 spectrometer operating at 500 MHz. For ^1H NMR, deuterated chloroform was used. MALDI-TOF measurements were run on a Bruker Autoflex II instrument using *trans*-2-[3-(4-*tert*-Butylphenyl)-2-methyl-2-propenylidene]malononitrile as a matrix. Dispersity values were measured using a Waters Breeze GPC system.

4.2 Calculation of Deuterium Integration %

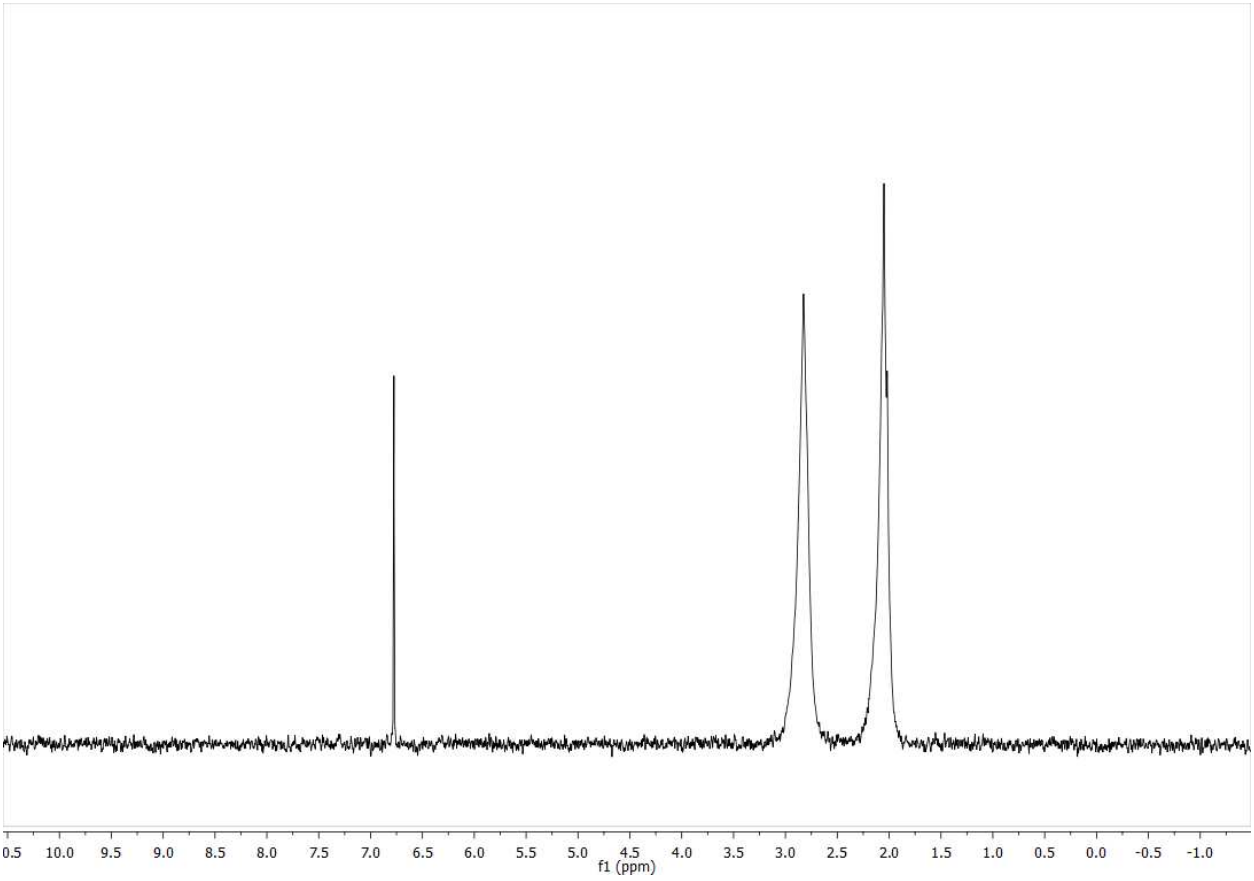

Figure 4.1. Example 2H NMR of deuterated product.

Calculated using ^{2}H NMR integration of the deuterated arene signal (I_P) against the signal of internal standard, deuterate acetone (I_A).

Deuterium integration % = $\frac{I_P}{I_A} \times \frac{0.1\ mmol}{0.18\ mmol \times 6} \times 100$

Equation 1. Deuterium Integration Calculation

4.3 Reaction Progress Kinetics Analysis (RPKA) – Same Excess[117]

RPKA Same Excess experiments were run by varying the starting concentrations of A & B, but keeping the difference between the two reagents consistent. All other reagents

concentrations were kept consistent across all reactions. The reactions were analyzed over time using GC-MS, observing for the formation of products **C**, **D**, & **E**. Using the collected information, the concentration of **A** remaining in the reaction mixture was plotted vs time. The plots of the lower starting concentrations (0.15 M and 0.1 M) were adjusted to match the timepoints of the 0.2 M reaction. The fact that the general trend is retained in all three plots suggests that there is no catalyst deactivation as the reaction progresses.

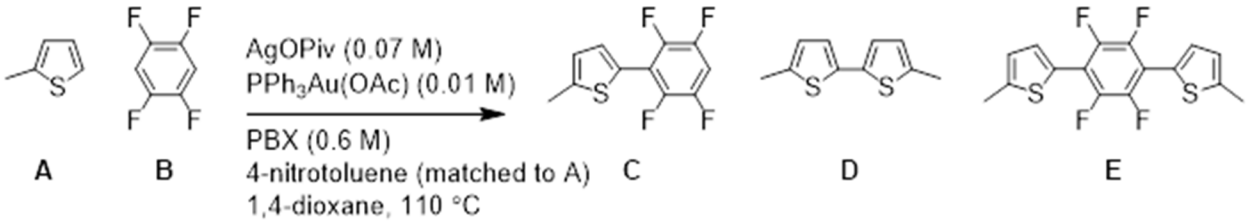

Figure 4.2. Reaction scheme for reaction progress kinetics analysis.

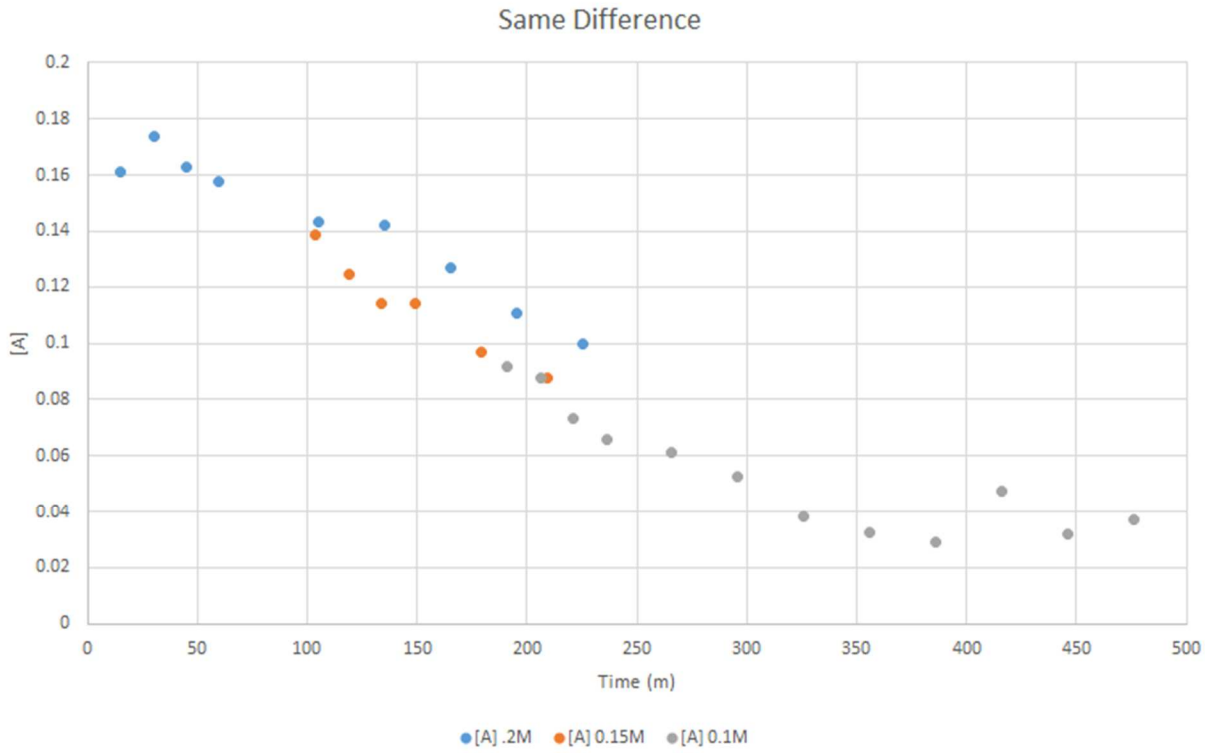

Figure 4.3. [A] vs. Reaction time plots overlay.

4.4 SPECTRAL DATA

4.4.1 *MALDI data*

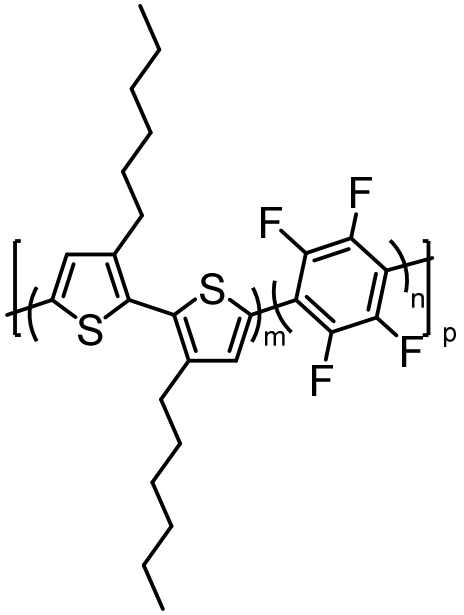

Figure 4.4. Polymer 1

Table 4.7. Notable M/Z values observed from MALDI of Polymer 1.
m and n were calculated using the known MW values of each monomer species.

M/Z	**m**	**n**
3253.7	8	4
3402.0	8	5
3476.1	10	1
3586.6	9	4
3734.8	9	5

3919.6	10	4
4067.8	10	5

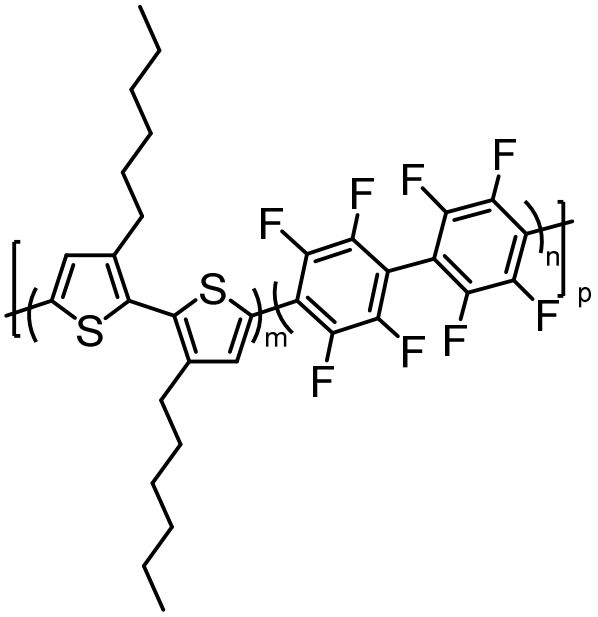

Figure 4.5. Polymer 2

Table 4.8. Notable M/Z values observed from MALDI of Polymer 2.
m and n were calculated using the known MW values of each monomer species.

M/Z	**m**	**n**
3181	6	4
3218	7	3
3514	7	4
3811	7	5
3847	8	4
4144	8	5

4.4.2 *^{1}H NMR*

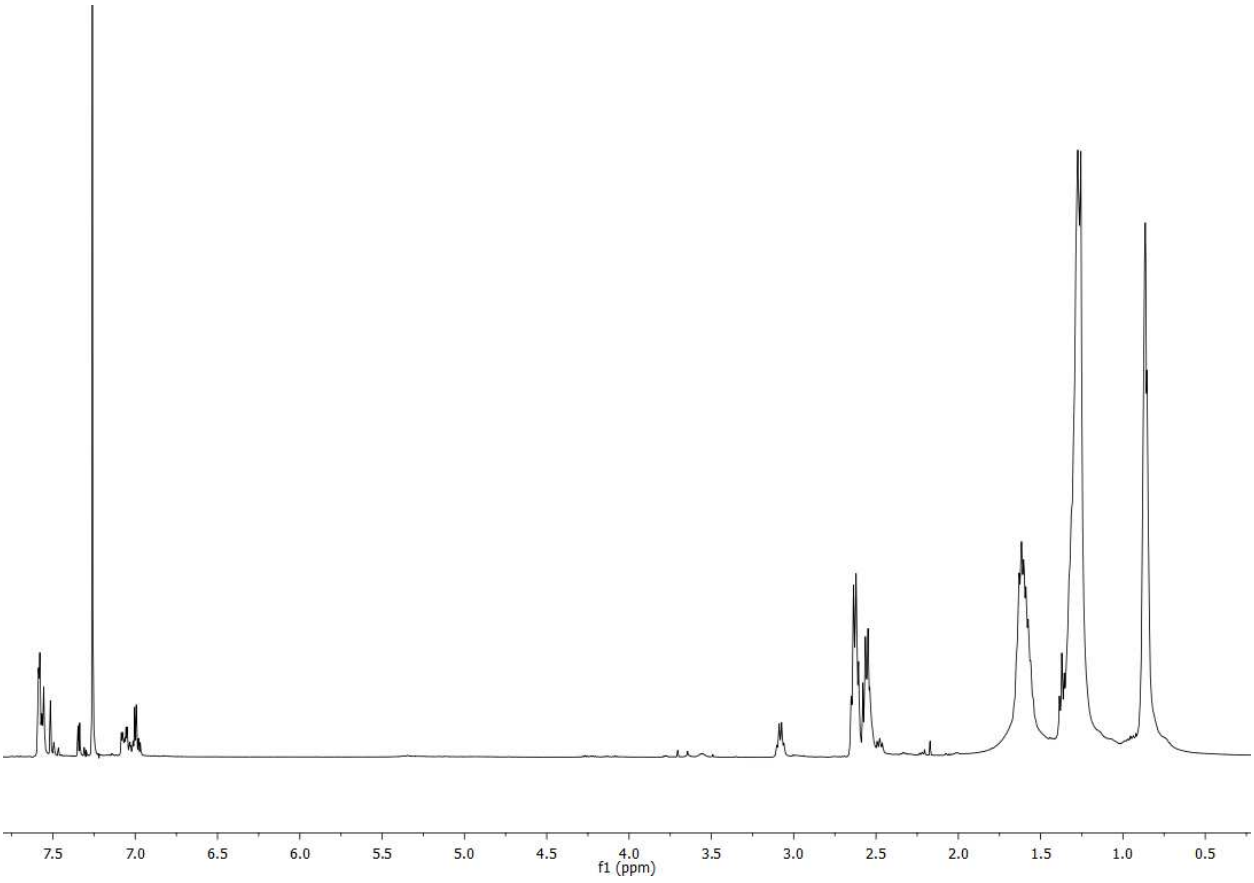

Figure 4.6. Example NMR spectrum of Polymer 1

^{1}H NMR (500 MHz, Chloroform-*d*) δ 7.57 (dd, *J* = 10.7, 5.4 Hz, 2H), 7.26 (s, 2H), 7.04 – 6.93 (m, 1H), 2.67 – 2.50 (m, 8H), 1.60 (ddq, *J* = 27.7, 15.7, 7.6 Hz, 12H), 1.41 – 1.21 (m, 28H), 0.91 – 0.73 (m, 15H).

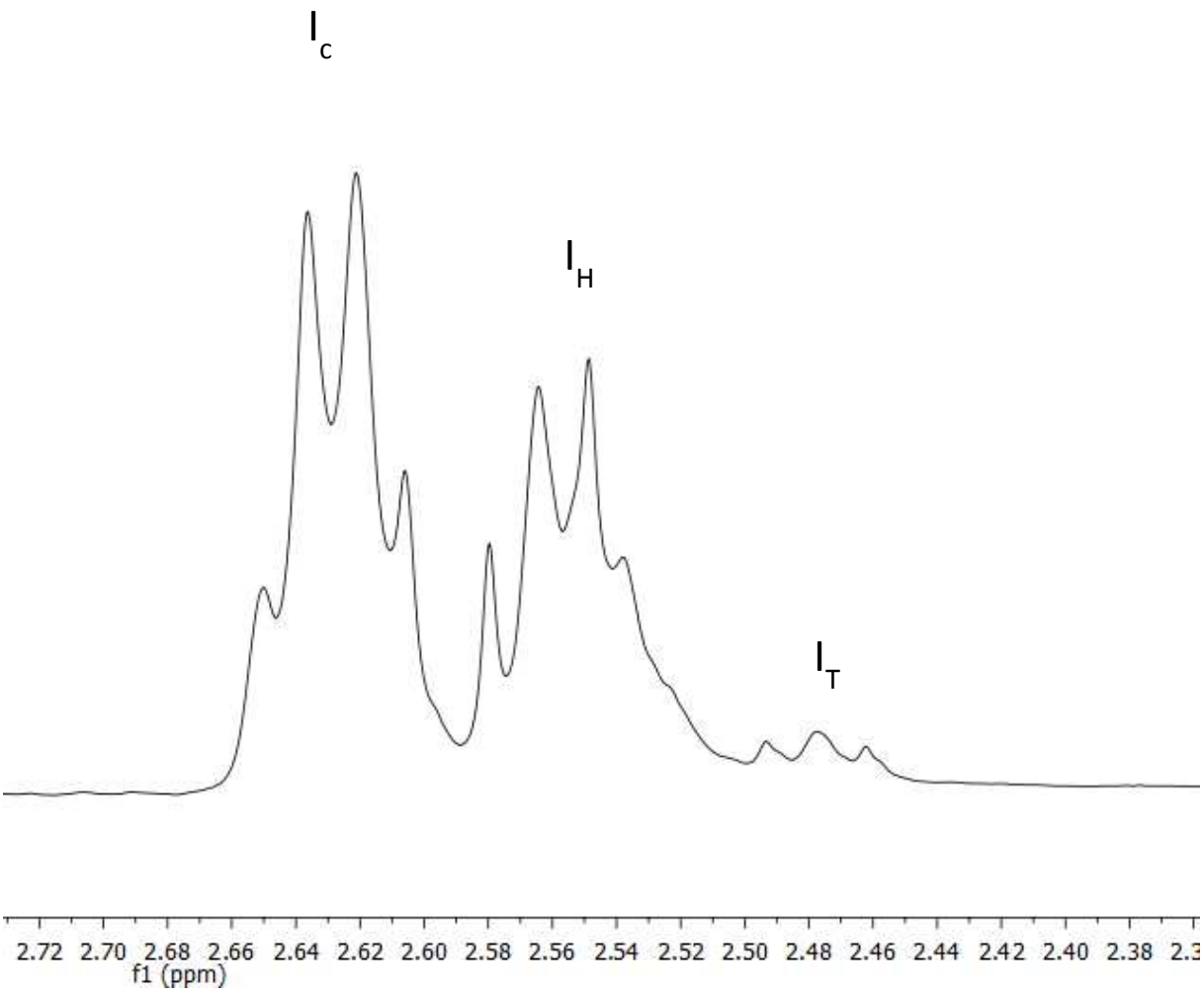

Figure 4.7. Region of NMR spectrum used to calculate % alt and M_n.

4.5 CALCULATING % ALT AND M_N USING ^{1}H NMR

$$\% \, alt = \frac{I_c}{I_c + I_H} * 100$$

Equation 2. % alt calculation.

$$M_n = \frac{I_C}{I_T}(MW_D/2 + MW_A/2) + \frac{I_H}{I_T} MW_D/2 + MW_D/2$$

Equation 3. M_n calculation, using end-group analysis.

APPENDIX B

Chapter 5. POLY(3-HEXYLTHIOPHENE) END-FUNCTIONALIZATION VIA QUENCHING RESULTING IN HETEROATOM-BOND FORMATION.

*The work in this chapter have previously been published: *Australian Journal of Chemistry* 69(7) 701-704 https://doi.org/10.1071/CH15790

5.1 ABSTRACT

End-functionalized poly(3-hexylthiophene) (P3HT) has contributed to continued advancements in conjugated polymer applications, especially within organic electronics. P3HT synthesized using Kumada Catalyst-Transfer Polycondesation (KCTP) has many favorable attributes such as controlled molecular weight, high regioregularity, and narrow dispersity. With the addition of reactive end-groups, P3HT plays an important role in advancing the development of hybrid materials and preparation of block copolymers. Exploring methods of end-functionalization that result in heteroatom-bond formation, giving a non-carbon atom bonded to the terminal thiophene, helps control and understand the p-n junction of hybrid materials. This research highlight focuses on the development of a novel and facile way of end-functionalizing P3HT with chalcogens.

5.2 INTRODUCTION

Within the growing field of organic electronics, P3HT is one of the most studied and understood organic semiconducting polymeric materials. Through the use of controlled Ni-

catalyzed cross coupling reactions, P3HT can be synthesized with controlled molecular weight and high regioregularity quite easily.[118,119] KCTP (Figure 5.1) is the most controlled method to synthesize P3HT. Using Ni-catalysts that stay associated with individual polymer chains results in living polymers that grow in a chain-growth manner. This means that the length of the polymer can be predicted and controlled using the ratio of monomer to catalyst loading. Upon quenching the polymerization, the resulting polymers should be within a small range of similar lengths, resulting in a low dispersity within the whole batch. The regioregularity of P3HT is controlled by using bi-functionalized monomer, building in selectivity for head-to-tail coupling throughout all of the Kumada cross-coupling reactions that take place during polymerization. P3HT also attracts attention due to positive characteristics, such as solution processability, desirable electronic properties, and relative stability.[120–126] With the addition of reactive end-groups, P3HT has played a role in developing conjugated copolymers and hybrid materials for electronic applications.[127–130] End-functionalized P3HT has contributed to advancements in surface modification of materials, such as nanowires and nanoparticles for organic electronic devices, by enhancing interactions between inorganic and organic semiconductors.[131] In the case of solar cells, there has been on-going interest in combining inorganic and organic materials, with the hopes of combining the positive attributes of both purely organic and purely inorganic solar cells. End-functionalized P3HT has played a key role in exploring such interests, because simply blending organic and inorganic materials has resulted in some challenges due to the formation of discrete domains.

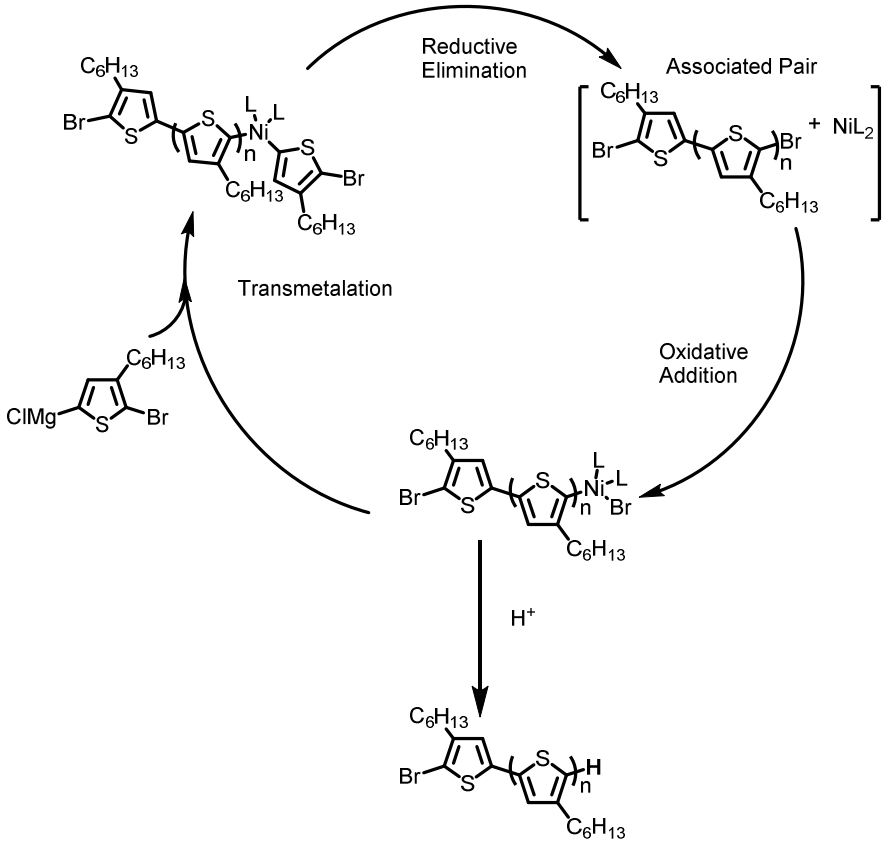

Figure 5.1. Kumada Catalyst-Transfer Polycondesation Mechanism.

Throughout the years, several ways of end-functionalizing P3HT have been developed and they can be sorted into three categories (Figure 5.2):

1. Initiators: Through the use of functional Ni-based initiators, in combination with KCTP, controlled functionalization of the α-end of P3HT has proven successful. Ni-based initiators designed with substituted aryl groups covalently attached are used to functionalize P3HT within the first Kumada cross-coupling reaction of the polymerization.[132–138] This method retains the controlled molecular weight and low polydispersity of P3HT synthesis. It also allows for exploring different polymer architectures, such as brush polymers. One of the disadvantages of this method is the synthesis of the externally prepared initiator. The purity of the initiator can affect the degree of functionality incorporated into P3HT. Also, the functional group on the initiator

needs to be chemically tolerant of the Grignard reagent on the monomer, therefore the scope of the end groups for this method is narrower and may require a protective group. This also means that the synthetic steps to deprotect the end-group needs to be compatible with the polymer, so as not to affect the performance of the resulting material.

2. Quenchers: Another method for end-functionalization of P3HT is the use of quenchers to add on desired functional groups. In the synthesis of unfunctionalized P3HT, an acid is readily used as a quencher to add a proton to the chain terminus. This method utilizes excess reagent of the desired functional group to quench the polymerization. Most of these reactions rely on a Grignard reagent to act as the quencher.[139–144] Depending on the reactivity of the quencher, the end-group may add to one end or both ends of P3HT. This method is advantageous because there is a broad range of functional Grignard reagents and other quenchers that have been developed. Most of the quenchers take advantage of the presence of the Ni-catalyst to facilitate the functionalization of the P3HT.

3. Post-polymerization: The third way that has been developed is post-polymerization modification.[145–148] This method requires multiple synthetic steps to add on the desired functional group and also has little control over which end is functionalized. This method relies on the activation of an aryl bromide bond or the installation of a functional group utilizing the Grignard metathesis method. This is disadvantageous because the necessity for more reactive chemicals to activate latent bonds and the reliance on multi-step syntheses result in increased waste products. Also, many of the chemicals required to activate these bonds require low temperature conditions. Reduced temperature can result in P3HT aggregations that may reduce performances in devices. The advantage of the post-polymerization modification method is that there are less limitations on

the functional groups, as the modifications to P3HT can be made after being isolated from the polymerization reactants, reducing the possibility of interfering reactions.

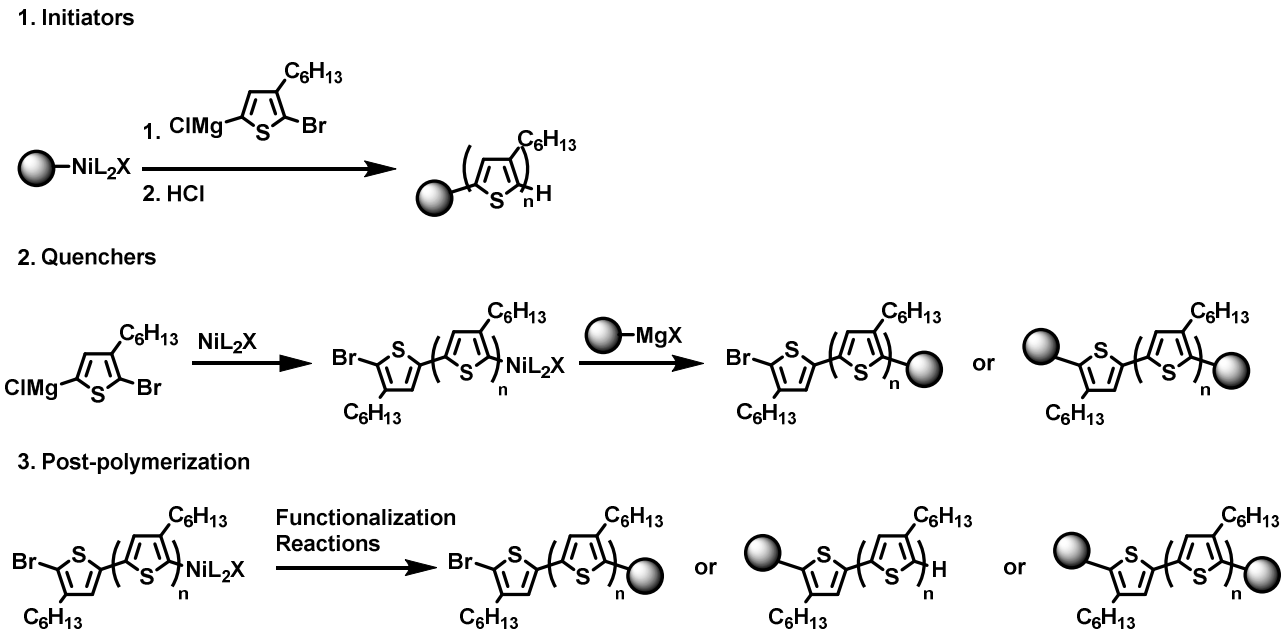

Figure 5.2. General schemes of three methods of end-functionalizing P3HT: initiators, quenchers, and post-polymerization.

Of the three developed methods, only a few examples exist for the installation of functional groups to the terminal thiophenes resulting in the formation of a bond between a heteroatom and carbon, such as C-Sn and C-P bonds.[131,148] Most are through the use of post-polymerization method, which means that the polymer is isolated with a C-Br bond, purified, and then functionalized through multi-step syntheses. This results in a large amount of waste and reduced yield of functionalized product. Interest in developing a method of quenching the reaction with compounds that can utilize the Ni-catalyst in such a way to install the desired functional group directly on to the terminal end of the polymer without the necessity of harsh chemicals has grown

due to reduction in waste. Such a method is also desirable because in combination with initiator end-functionalization, P3HT can be tailored to result in discretely functionalized ends of the polymer, resulting in two different end-groups on each P3HT chain. Such control of individual ends of P3HT can have an effect on the overall morphology of the material.

A major challenge in organic-inorganic hybrid solar cells is the control over the bulk morphology and interfacial structures of nanoparticles within organic polymer matrices, when blended together as an active layer. Depending on the surface properties of the nanoparticles and the interactions with the organic polymer, microscopic phase separation can occur. If these phase separations are larger than exciton diffusion lengths, charge recombination will be favored over charge separation. One of the ways to address this problem, is to increase the interaction between the donor and acceptor components, to improve charge dissociation. A step that has been taken towards improving such interactions has been grafting organic semiconducting polymers directly onto the surface of nanoparticles. This has been achieved by installing desired functional groups on the organic semiconducting polymers to improve interaction with targeted inorganic materials. Incorporation of the proper functional end groups can result in high surface coverage of the nanoparticle due to strong interactions, a direct electronic coupling between the inorganic and organic components, and a defined donor/acceptor interface. For example, Kruger and coworkers were able to improve interactions between TiO_2 and P3HT by functionalizing P3HT with cyanoacetic groups. A blend material of the unfunctionalized-P3HT/TiO_2 had a PCE of 0.1%, while monofunctionalized- P3HT/TiO_2 had a PCE of 0.2%, and bifunctionalized- P3HT/TiO_2 had a PCE of 2.2%.[130] Grafting polymer onto the surface of nanoparticles seems to improve the performance in two different ways. Grafting semiconducting polymer onto the surface of inorganic nanoparticles/nanowires increases the dispersity of the inorganic material throughout the matrix

of the polymer and facilitates formation of doner/acceptor interface on the nanoscale to encourage charge transfer and transport in the hybrid material.[129]

Heteratom-bond formation has played a role in increasing the understanding of the interactions at the p-n junction in organic/inorganic hybrid systems. For example, by using phosphonic ester terminated P3HT, Briseno and coworkers were able to graft P3HT onto ZnO nanowires and build individual scale devices to understand optoelectronic properties and morphologies of the bulk material within a device.[131] By increasing the number of functional groups that can be installed directly to the terminal thiophene, the overall understanding of hybrid material morphologies and electrical properties can be improved.

5.3 Results and Discussion

Chalcogens are end-groups of interest due the possibility of improved donor/acceptor interactions as described above. Thiols have been shown to interact with many metal surfaces, such as Ag, Au, CdSe, CdS, and Zn.[149] This shows great potential in grafting chalcogen functionalized P3HT onto nanoparticles or nanowires to result in hybrid materials for solar cell applications.

A prime example of installing a heteroatom end-group onto P3HT utilizing a quencher was achieved by Luscombe et al.[150] wherein elemental sulfur was reacted in the presence of 1,8-Diazabicyclo[5.4.0]undec-7-ene (DBU) to install thiols exclusively on the ω-end of P3HT. The same method was also utilized to install selenol groups on the ω-end of P3HT using Selenium powder and DBU. A similar method, using a solution of triisopropylsilanethiol (TIPS-SH) and isopropylmagnesium (iPrMgCl) chloride as a quencher, results in thiol termination of both the α- and ω-ends of P3HT (Figure 5.3). The combination of initiator and quencher methods was also

demonstrated by adding a tolyl group to the α-end and a thiol to the ω-end of the polymer (Scheme 4).

Using elemental sulfur and DBU results in only one end of the polymer being functionalized, due to the nature of the quencher. Unlike in the case of some Grignard metathesis based quenchers, the Ni-catalyst does not reinsert into the C-Br bond on the α-end of the P3HT. Therefore, even without the presence of an initiator, the thiol group is only added to the ω-end of the polymer. When combined with an initiator, two discrete functional groups can be added to either end of the P3HT. When using TIPS-SH and iPrMgCl, the Ni-catalyst does interact with the α-end of the P3HT, resulting in bis-thiol termination. The advantage of the TIPS-SH and iPrMgCl method is the protection of the thiol group that can be deprotected under mild conditions as needed.

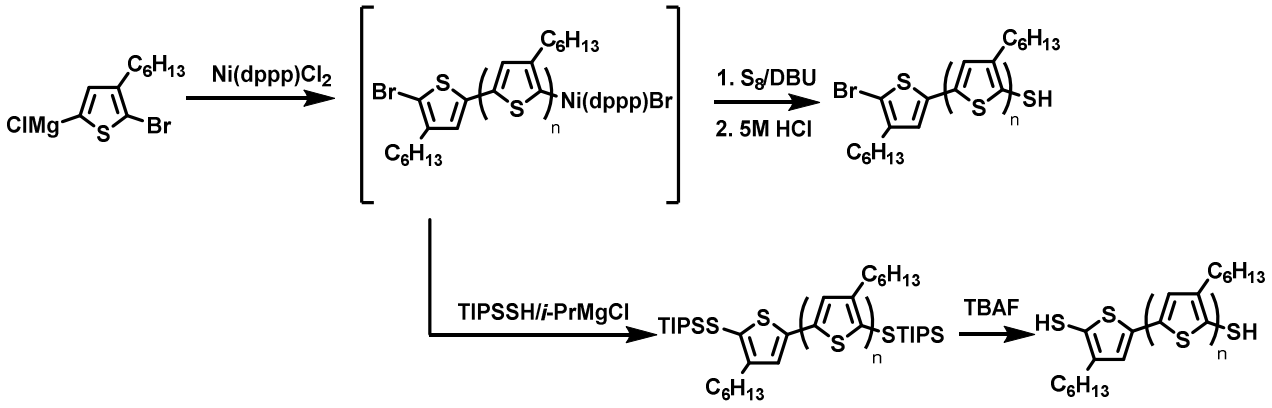

Figure 5.3. Mono and bis-thiol end-functionalization of P3HT.

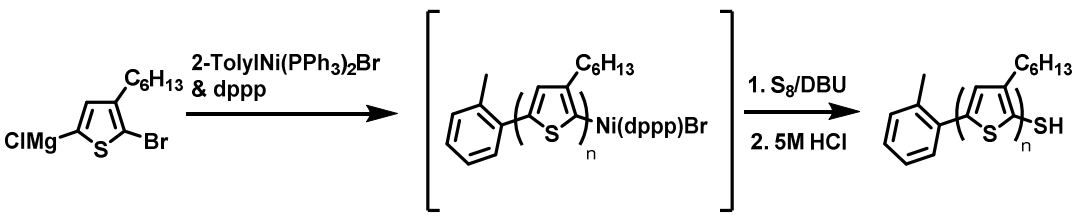

Figure 5.4. Combination of initiator and quencher to yield discrete functionalities on either end of P3HT

5.4 CONCLUSION

By expanding the number of functional groups that can be installed by heteroatom bond-forming quenchers, P3HT can be functionalized in an energy efficient way, resulting in direct functionalization of the terminal thiophene. This could be achieved using mild temperature and less chemical loading, resulting in less waste. Developing this technique further can increase the possible combinations of initiators and quenchers to result in controlled functionalization of each end independently, giving rise to two different functional groups on each chain of P3HT. The resulting material could be utilized to further advancement in organic electronics, by contributing to surface modification and development of hybrid materials, with controlled morphologies. Expanding the diversity of functional groups that can be added this way should directly influence the development of hybrid materials, by aiding the direct ligation of P3HT to the inorganic components of the hybrid material.

VITA

PROFESSIONAL EXPERIENCE

2013-Present	**Ph.D. Candidate in Chemistry** *University of Washington* ·Execute research focused on polymer synthesis methodology, applying C-H functionalization toward organic solar cell materials.
2011-2013	**Research Technician** *Aeonclad Coatings* ·Successfully developed and implemented an RF-induced plasma coating technique for waterproofing down for Patagonia, resulting in the pilot production of Encapsil down. ·Managed team of 11 technicians during pilot production.
2008-2012	**Student Research Assistant** *University of Texas at Austin* ·Performed research focusing on polymer functionalization for fuel cell membrane materials.
2008	**Student Research Assistant** *University of Texas at Arlington* ·Engaged in focused methodology research of a catalytic Wittig reaction.

AWARDS & FELLOWSHIPS

2018	Clean Energy Institute – Outreach & Service Award
2018	Husky 100
2018	Center for Selective C-H Functionalization Poster Presentation Award - 2nd Place
2017	Pacific Science Center Science Communication Fellowship
2015	Clean Energy Institute Fellowship
2008	Undergraduate Research Fellowship

LEADERSHIP & CIVIC ACTIVITIES

2017-Present **Organizer**
Strategies for Cultivating Inclusion in STEM (SCI-STEM)
· Contribute to planning of full-day event focused on inclusion.
· Coordinate with potential speakers and workshop organizers.

2017-Present **Science Communication Fellow**
Pacific Science Center
· Designed and prototyped museum activity related to polymer research
· Executed museum activity in varied settings with all age groups

2016-2018 **Lead Officer**
Diversity in Clean Energy
· Organize career talks with professionals in the clean energy field.
· Arrange professional development workshops for students.

2016-2017 **Tutor**
Science Explorers
· Facilitated hands-on experiments with local elementary students.

2016 **Instructor**
Center for Enabling New Technologies through Catalysis
· Presented and instructed hands-on lab pertaining to energy at local high schools.

2015-Present **Fellow**
Clean Energy Institute
· Assisted at numerous local science and education fairs with hands-on activities.
· Designed and executed lesson for local middle school afterschool program.
· Contributed to education material for Clean Energy Institute undergraduate summer program.

2015 **Mentor**
Alliances for Learning and Vision for Underrepresented Americans
· Mentored underrepresented student with interest in STEM in the laboratory setting and with science communication.

2014-2015 **Mentor**
Gifted Program at Interlake High School
· Advised local high student during her internship in the laboratory.

2014 **Mentor**
National Science Foundation Research Experience and Mentoring
· Mentored underrepresented student with interest in STEM in the laboratory setting and with science communication.

COMMUNICATION

Presentations

2018	Center for Selective C-H Functionalizaion – National Science Foundation Annual Meeting – Atlanta, GA.
2017	International Symposium on Functional π-Electron Systems – Hong Kong, China.
2017	Center for Selective C-H Functionalizaion – National Science Foundation Annual Meeting Atlanta, GA.
2016	Orcas International Conference on Energy Conversion – Friday Harbor, WA.
2016	Virtual Institute for C-H Functionalization International Workshop – Osaka & Nagoya, Japan.
2016	Center for Selectice C-H Functionalization – National Science Foundation Site Visit – Atlanta, GA.
2015	International Symposium on Functional π-Electron Systems – Seattle, WA.
2015	US-Japan Workshop on Advances in Organic/Inorganic Hybrid – Seattle, WA.
2014	Orcas International Conference on Energy Conversion – Friday Harbor, WA.

Publications

2018	"Exploration and Development of Gold- and Silver-catalyzed Cross Dehydrogenative Coupling Toward Donor-Acceptor π-conjugated Polymer Synthesis" *Manuscript Submitted*
2018	"Recent Developments in C–H Activation for Materials Science in the Center for Selective C–H Activation" *Molecules* **2018**, *23*, 922-934
2016	"Poly(3-hexylthiophene) End-functionalization via Quenching Resulting in Heteroatom-bond Formation" *Aust. J. Chem*., **2016**, *69*, 701-704.
2015	"N-type Hyperbranched Polymers for Supercapacitor Cathodes with Variable Porosity and Excellent Electrochemical Stability" *Macromolecules*, **2015**, *48*, 5196-5203.
2013	"Part I: The Development of the Catalytic Wittig Reaction" *Chem. Eur. J.* **2013**, *19*, 15281-15289.
2009	"Recycling the waste: The development of a catalytic Wittig reaction." *Angewandte Chemie*, **2009**, *48*, 6836-6839.